


Review

A Review of Hydrogen Production via Seawater Electrolysis: Current Status and Challenges

Yixin Zhang ^{1,†}, Yu Zhang ^{1,†}, Zhichuan Li ^{2,†}, Ende Yu ³, Haibin Ye ², Zihang Li ², Xinshu Guo ², Daojin Zhou ⁴, Cheng Wang ^{5,*}, Qihao Sha ^{4,*} and Yun Kuang ^{3,6,*} 

¹ School of Chemistry and Chemical Engineering, Southwest Petroleum University, Chengdu 610500, China; yixinzhang_edu@163.com (Y.Z.); yuzhang5316_edu@163.com (Y.Z.)

² Cnooc Energy Technology & Service Limited, Clean Energy Branch, Tianjin 300467, China; lizhch6@cnooc.com.cn (Z.L.); yehb@cnooc.com.cn (H.Y.); lizh20@cnooc.com.cn (Z.L.); guoxsh6@cnooc.com.cn (X.G.)

³ Ocean Hydrogen Energy R&D Center, Research Institute of Tsinghua University in Shenzhen, Shenzhen 518057, China; yuende2020@163.com

⁴ State Key Laboratory of Chemical Resource Engineering, Beijing Advanced Innovation Center for Soft Matter Science and Engineering, College of Chemistry, Beijing University of Chemical Technology, Beijing 100029, China; zhoudj@mail.buct.edu.cn

⁵ Basin Research Center for Water Pollution Control, Research Academy of Environmental Sciences, Beijing 100012, China

⁶ Hydrogen Storage and Separation R&D Centre, Research Institute of Tsinghua University in Shenzhen, Shenzhen 518057, China

* Correspondence: wang.cheng@craes.org.cn (C.W.); shaqh@buct.edu.cn (Q.S.); kuangy@tsinghua-sz.org (Y.K.)

† These authors contributed equally to this work.

Abstract: Seawater electrolysis represents a promising green energy technology with significant potential for efficient energy conversion. This study provides an in-depth examination of the key scientific challenges inherent in the seawater-electrolysis process and their potential solutions. Initially, it analyzes the potential issues of precipitation and aggregation at the cathode during hydrogen evolution, proposing strategies such as self-cleaning cathodes and precipitate removal to ensure cathode stability in seawater electrolysis. Subsequently, it addresses the corrosion challenges faced by anode catalysts in seawater, introducing several anti-corrosion strategies to enhance anode stability, including substrate treatments such as sulfidation, phosphidation, selenidation, and LDH (layered double hydroxide) anion intercalation. Additionally, this study explores the role of regulating the electrode surface microenvironment and forming unique coordination environments for active atoms to enhance seawater electrolysis performance. Regulating the surface microenvironment provides a novel approach to mitigating seawater corrosion. Contrary to the traditional understanding that chloride ions accelerate anode corrosion, certain catalysts benefit from the unique coordination environment of chloride ions on the catalyst surface, potentially enhancing oxygen evolution reaction (OER) performance. Lastly, this study presents the latest advancements in the industrialization of seawater electrolysis, including the in situ electrolysis of undiluted seawater and the implementation of three-chamber dual anion membranes coupled with circulating electrolyte systems. The prospects of seawater electrolysis are also explored.

Keywords: hydrogen production; seawater splitting; cathodic stability; anti-corrosion strategies; industrialization



Citation: Zhang, Y.; Zhang, Y.; Li, Z.; Yu, E.; Ye, H.; Li, Z.; Guo, X.; Zhou, D.; Wang, C.; Sha, Q.; et al. A Review of Hydrogen Production via Seawater Electrolysis: Current Status and Challenges. *Catalysts* **2024**, *14*, 691. <https://doi.org/10.3390/catal14100691>

Academic Editors: Loreta Tamasauskaite-Tamasiunaite and Virginija Kepeniene

Received: 26 July 2024

Revised: 20 September 2024

Accepted: 1 October 2024

Published: 4 October 2024



Copyright: © 2024 by the authors. Licensee MDPI, Basel, Switzerland. This article is an open access article distributed under the terms and conditions of the Creative Commons Attribution (CC BY) license (<https://creativecommons.org/licenses/by/4.0/>).

1. Introduction

Hydrogen plays a pivotal role in the global energy transition as a clean and efficient energy carrier. The combustion of hydrogen produces only water, emitting no greenhouse gases or pollutants, making it a crucial component of the future energy system [1]. However, current large-scale hydrogen production technology via water electrolysis faces

several challenges, the most significant being the shortage of freshwater resources. Freshwater resources are essential for human survival and development; however, they are unevenly distributed globally, leading to severe shortages in many regions. Therefore, it is crucial to find an alternative electrolysis medium to freshwater to promote large-scale hydrogen production globally. Seawater, the most abundant water resource on Earth, covers approximately 71% of the planet's surface and has nearly inexhaustible reserves. Consequently, using seawater for hydrogen production via electrolysis has become an attractive option. If efficient seawater electrolysis can be realized, it will not only alleviate pressure on freshwater resources but also fully utilize Earth's abundant natural resources, providing humanity with a continuous supply of clean energy [2]. The successful industrial application of seawater electrolysis will bring multiple benefits. Firstly, it will significantly reduce pressure on freshwater resources and provide humanity with a clean energy source for sustainable development. Furthermore, seawater electrolysis for hydrogen production can be integrated with offshore wind power, offshore solar power, and other renewable energy sources to create a novel clean energy production system [3]. Additionally, hydrogen produced from seawater electrolysis can be directly used for energy supply in ships, offshore platforms, and other marine facilities, further promoting the development of the marine economy.

Although seawater electrolysis for hydrogen production is promising, its realization faces numerous challenges and issues. Firstly, seawater contains numerous salts, impurities, and microorganisms, which can cause electrode corrosion, impede electrolysis efficiency, and produce by-products that affect the stability of the electrolysis process. Secondly, chlorine ions in seawater can easily generate chlorine gas during electrolysis, which not only causes equipment corrosion but also poses toxicity risks, necessitating effective measures to prevent chlorine gas generation and release [4,5].

Additionally, the high conductivity and complex chemical composition of seawater increase the difficulty in designing and operating electrolysis equipment [4]. To address these challenges, scientists have proposed various strategies to improve the efficiency and stability of seawater electrolysis. Firstly, researchers have developed new electrode materials and catalysts to enhance the efficiency of the electrolysis reaction and improve the corrosion resistance of the electrodes. Secondly, by optimizing the electrolysis process, such as using bipolar electrolysis and membrane separation technology, by-product generation can be effectively reduced, thereby improving the safety and stability of the process. Additionally, some studies have explored adding specific additives to the electrolysis process to inhibit the attack of Cl^- on the anode substrate, thereby improving the stability of seawater electrolysis electrodes [5–7].

This review will explore in detail the coping strategies and recent advances in seawater electrolysis for hydrogen production from multiple perspectives. Firstly, we will introduce new electrode materials and catalysts used in seawater electrolysis and analyze their advantages in enhancing electrolysis efficiency and corrosion resistance [4,5]. Secondly, we will discuss the optimization measures of the electrolysis process. Additionally, we will introduce some of the latest industrial tools, such as the design and application of offshore electrolysis platforms for hydrogen production. By elaborating on these topics, we aim to provide valuable references and guidance for the development of seawater electrolysis hydrogen production technology [2,8].

2. Self-Cleaning Cathodic Anti-Precipitation and Seawater Magnesium-Extraction Techniques

The concentrations of the main metal elements in seawater are as follows: Na (10800 ppm), Mg (1290 ppm), Ca (413 ppm), K (400 ppm), Ni (0.18 ppm), Fe (0.005 ppm), and U (0.0034 ppm). The primary metal ions in seawater are Na^+ , Mg^{2+} , Ca^{2+} , and K^+ , with Mg^{2+} and Ca^{2+} having the most significant impact on electrode performance during seawater electrolysis [9]. One of the main problems faced by seawater electrolysis cathodes is that during the continuous cathodic hydrogen precipitation reaction, the cathode produces a large amount of OH^- [10,11].

This OH^- reacts with the free calcium and magnesium ions in seawater, forming sediments on the electrode surface [12]. During seawater electrolysis, Mg^{2+} and Ca^{2+} significantly impact electrode performance by forming precipitates on the electrode surface, which block active sites and hinder the diffusion and transfer of substances in the electrocatalytic process.

As the hydrogen evolution reaction (HER) proceeds continuously ($2\text{H}_2\text{O} + 2\text{e}^- \rightarrow \text{H}_2 + 2\text{OH}^-$), it leads to a localized increase in the concentration of OH^- at the cathode surface. A substantial amount of OH^- will precipitate ($\text{M}^{2+} + 2\text{OH}^- \rightarrow \text{M}(\text{OH})_2$, where M^{2+} represents either Ca^{2+} or Mg^{2+}). Due to strong intermolecular forces, including van der Waals forces and contact adhesion forces, these precipitates tend to adhere to the electrode surface. Since the formation of magnesium hydroxide requires a pH of approximately 9.3, and the formation of calcium hydroxide requires a pH of around 12.0, maintaining the electrolyte pH near 9.3 may facilitate the co-production of magnesium hydroxide at the cathode [13].

These sediments strongly interact with the solid interface of the electrode due to van der Waals forces and adhesion forces [14], ultimately forming a difficult-to-remove precipitate. This not only blocks the catalytic active sites but also leads to a rapid decrease in electrolysis efficiency and current density [2,15,16]. The high concentration of impurity ions in seawater and the lack of an effective precipitation-rejection mechanism exacerbate the precipitation problem. This leads to decreased electrode activity and electrolysis efficiency and necessitates high overpotentials during the electrolysis process, increasing energy consumption. These challenges limit the industrial application and large-scale deployment of seawater electrolysis technology. Precipitates formed in situ during electrolysis tend to bind to the solid interfaces on the electrode surface. This hinders the active sites, reduces the electrode working area, drastically decreases the current density, and ultimately affects hydrogen release.

Magnesium ions (Mg^{2+}) combine with hydroxide ions (OH^-) to form a precipitate at a lower pH than calcium ions (Ca^{2+}). In addition, if calcium hydroxide ($\text{Ca}(\text{OH})_2$) has already formed, the following substitution reaction can occur in the presence of magnesium ions in seawater: $\text{Mg}^{2+} + \text{Ca}(\text{OH})_2 \rightarrow \text{Mg}(\text{OH})_2 + \text{Ca}^{2+}$. This reaction shows that magnesium ions can react with calcium hydroxide to form a magnesium hydroxide ($\text{Mg}(\text{OH})_2$) precipitate and calcium ions even when calcium hydroxide has already formed [17]. This property makes it possible to extract magnesium from seawater because the formation of magnesium hydroxide takes precedence over the formation of calcium hydroxide, thus increasing magnesium recovery during seawater extraction.

In a recent breakthrough, Tang et al. designed and constructed an innovative microscopic bubble/precipitate traffic system (MBPTS) [18], which significantly reduces the overpotential and improves anti-precipitation performance by combining the highly efficient hydrogen precipitation material NiCoP with a honeycomb 3D porous carbon framework. In this process, hydrogen, after being generated from the catalytic sites of NiCoP, flows continuously along the carefully designed channels of the porous carbon material, creating homogeneous localized gas streams. These gas streams act as finely tuned cleaning agents, continuously pushing and removing the precipitates adhering to the cathode surface, achieving self-cleaning during the electrolysis process.

The electrode structure is characterized by its porosity and regularity, which facilitates the continuous generation of uniformly sized hydrogen bubbles (Figure 1a,b). These bubbles are uniformly and consistently expelled from the electrode surface, effectively preventing precipitate formation and ensuring stable long-term electrode performance. Even in seawater conditions, NCP/PC materials favorably dissociate into H_{ads} thermodynamically, offering densely distributed active sites conducive to rapid reactions (Figure 1c). Consequently, NCP/PC materials maintain high θ_{H} coverage levels, releasing substantial quantities of hydrogen while repelling precipitates. This design not only enhances the efficiency of seawater electrolysis but also resolves persistent cathode precipitation challenges, providing robust technical support for industrial-scale hydrogen production from seawater.

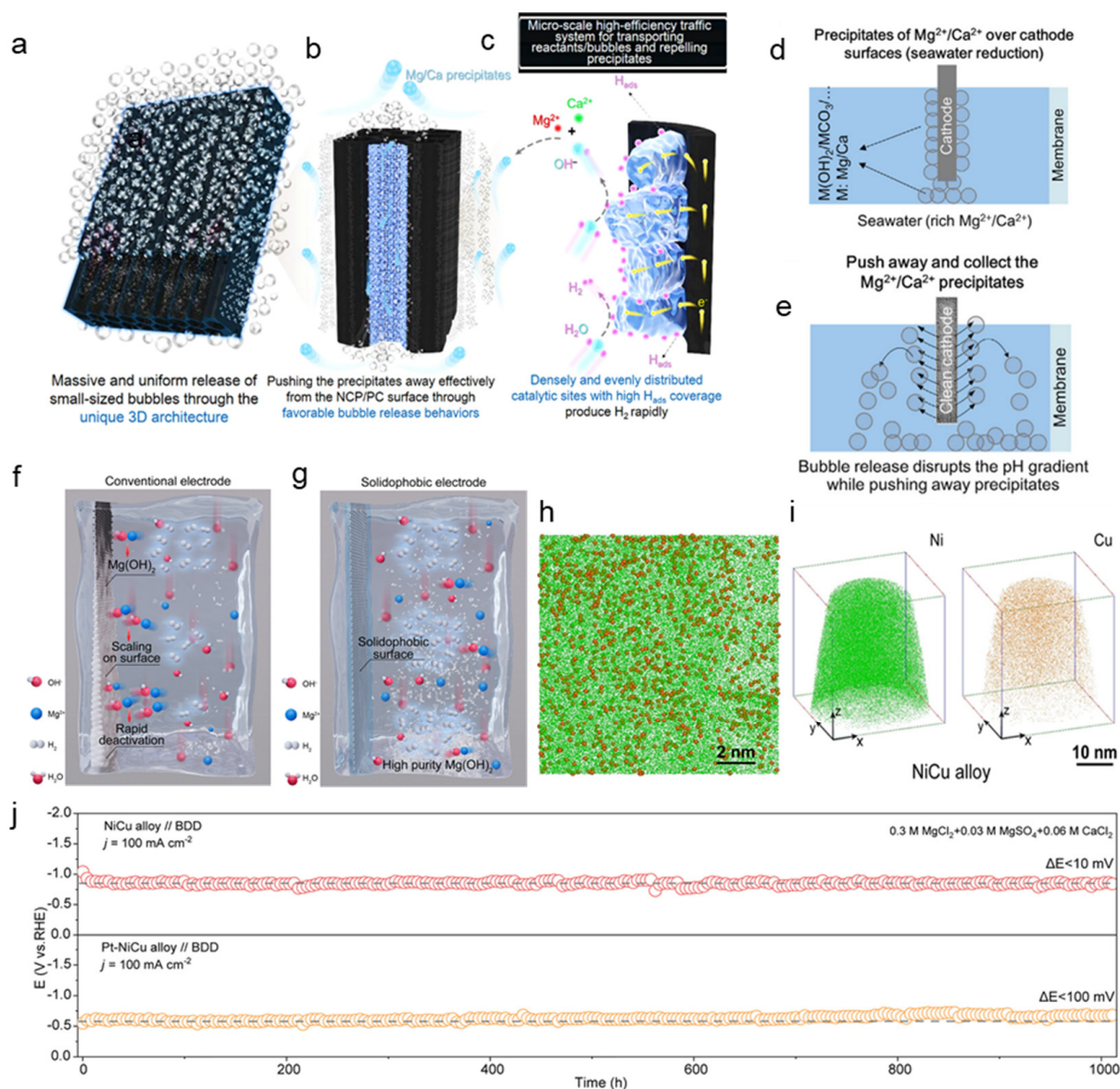


Figure 1. Self-cleaning cathodic antiprecipitation and seawater magnesium-extraction techniques. (a–c) Schematic diagrams of efficient traffic of bubbles and precipitates on/in the NCP/CP. The bubble acts as the cleaner to make NCP/CP free from precipitation by repelling precipitates without a break; (d) Surface of the cathode for electrocatalytically reducing alkaline seawater is clean; (e) Natural seawater reduction causes local pH to rise, which causes Mg^{2+}/Ca^{2+} to precipitate and attach onto the cathode surface; (f,g) Schematic illustration of natural seawater electrolysis on a conventional cathode and solidophobic cathode.; (h) Higher-magnification views of Cu atoms in Ni matrix; (i) APT ion distribution maps of Ni and Cu; (j) Long-term accelerated durability tests of NiCu alloy and Pt-NiCu alloy electrode under 100 mA cm^{-2} .

In another groundbreaking study, Tang’s team further explored and proposed three effective strategies to mitigate surface precipitation issues: the proton sponge [19], external flow field, and self-cleaning cathode. These strategies collectively form an innovative approach to produce nanoscale $Mg(OH)_2$ and high-purity hydrogen. The proton sponge disrupts the local pH gradient formed on the cathode surface; the external flow field physically removes precipitates from the cathode surface; and the self-cleaning cathode reduces precipitate accumulation, thereby minimizing its impact on the electrolysis process. During seawater electrolysis, abundant Ca^{2+} and Mg^{2+} in seawater tend to precipitate on the cathode (Figure 1d). However, the introduction of a self-cleaning cathode not only

reduces precipitate accumulation on the cathode but also allows the hydrogen generated at the cathode to help remove surface precipitates and regulate the local pH gradient (Figure 1e). These research findings not only provide new perspectives and solutions for the development of seawater electrolysis technology but also open new avenues for the efficient production and utilization of green energy. They hold significant potential for contributing to future energy transitions.

During seawater electrolysis, strong intermolecular interactions between solids, particularly van der Waals forces and adhesion, cause $\text{Mg}(\text{OH})_2$ to adhere to the electrode surface, leading to fouling. This results in a rapid reduction in the electrode's active area and current density (Figure 1f). Thus, preventing the adhesion of $\text{Mg}(\text{OH})_2$ to the electrodes (Figure 1g) is a crucial challenge in seawater electrolysis for magnesium extraction and hydrogen production.

Yi et al. recently made groundbreaking progress in the field of cathodic precipitation resistance for seawater electrolysis [13]. They successfully synthesized a NiCu alloy electrode with high surface energy and excellent hydrogen evolution reaction (HER) activity. The distribution of copper within the nickel matrix is highly disordered (Figure 1h,i). This unique structural design significantly increases the surface disorder of the alloy, thereby effectively enhancing its surface energy [20]. This high surface energy characteristic promotes the formation of a dense adsorbed water layer through its hydrogen-bond network, substantially raising the energy barrier for magnesium ion penetration, thus preventing magnesium ions from reaching the electrode surface [21,22]. Consequently, magnesium ions are more likely to nucleate homogeneously with hydroxide ions in the solution phase rather than heterogeneously on the electrode surface.

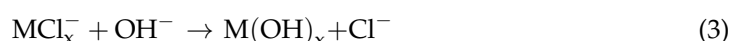
Due to these properties of the NiCu alloy, this catalyst demonstrates outstanding stability in salt solutions with extremely high concentrations of Mg^{2+} and Ca^{2+} (7.9 g/L and 2.4 g/L, respectively, approximately 10 times the concentrations found in natural seawater), and can stably operate for over 1000 h. During the 1000 h test period, the voltage decay of the NiCu alloy was less than 10 mV, while the voltage loss of the Pt-NiCu alloy was less than 100 mV (Figure 1j). Additionally, under actual seawater conditions, this cathode not only efficiently produces high-purity hydrogen but also generates an $\text{Mg}(\text{OH})_2$ by-product with purity exceeding 99%, achieving dual high-purity product generation in seawater electrolysis. This accomplishment not only demonstrates the electrode's stability under high-concentration electrolyte conditions but also provides a new and efficient solution to the cathodic precipitation problem in seawater electrolysis, promising further advancements in green hydrogen production and resource recovery.

In the development of seawater electrolysis as a clean energy technology, the anti-precipitation capability of the cathode is crucial. If we can efficiently co-produce high-purity, environmentally friendly, and economically valuable $\text{Mg}(\text{OH})_2$ while generating hydrogen at the cathode [13], this would not only significantly reduce the operating costs of seawater electrolysis but also greatly enhance its market competitiveness compared to other water electrolysis methods. Through innovative design, combining high-activity HER catalysts, high surface energy cathodes, self-cleaning functions, and the synergistic effects of external flow fields [18,19], a solid step has been taken toward the industrial development of seawater electrolysis technology. These groundbreaking advancements not only solve the long-standing precipitation problem in seawater electrolysis but also open up new possibilities for realizing green, efficient, and economical utilization of seawater resources.

3. The Strategies of Anodic Anti-Corrosion

Direct seawater electrolysis faces the challenge of competition between the chloride evolution reaction (CER) and the oxygen evolution reaction (OER). The CER is a two-electron-transfer process, whereas the OER involves a four-electron transfer, making the side reaction CER kinetically favorable over OER [23]. Thermodynamically, in the lower pH range, the thermodynamic barrier increases progressively with the rise in pH, accompanied by the formation of hypochlorite. When the pH exceeds 7.5, the chlorine evolution reaction

occurs, and the thermodynamic barrier reaches its maximum, with a potential difference of 480 mV [24]. During the direct electrolysis of seawater, chloride ions also tend to adsorb on the anode, forming metal-chloride coordination, which corrodes the anode substrate and leads to electrode deactivation (as shown in Equations (1) to (3)) [25]. Moreover, local pH fluctuations at the electrode surface may reduce the potential window at high current densities. Therefore, for efficient seawater electrolysis, it is necessary to carry out the OER at high pH (~14.0) to achieve the minimum overpotential, enabling high current density water splitting and promoting seawater electrolysis.



Furthermore, Lu et al. found that, in addition to chloride ions corroding the anode, Br^- also significantly affect electrode durability [4]. Through experimental and simulation studies, they discovered that Cl^- tends to cause localized deep and narrow corrosion pits, while Br^- leads to extensive shallow and wide corrosion pits. The different corrosion mechanisms of various halide ions result in different corrosion behaviors: Cl^- produces localized deep and narrow pitting corrosion, while Br^- causes large-area delamination of the catalyst layer, forming shallow and wide corrosion pits on the substrate. Density Functional Theory (DFT) calculations revealed that Cl^- has the lowest energy barrier (compared to Br^-) to overcome during the penetration process from the surface to the lattice, indicating that Cl^- is more likely to enter the lattice interior. For Ni-based substrates, in a chlorine-containing environment, the initial reaction typically involves the formation of NiO, leading to the thickening of the passivation layer. Cl^- is difficult to react with the passivation layer, but it easily diffuses into the lattice interior, thus forming narrow and deep pitting corrosion along the vertical direction of the electrode. In contrast, Br^- is less likely to penetrate the lattice and tends to undergo corrosion reactions at multiple sites, resulting in the formation of wide and shallow corrosion pits along the horizontal direction of the electrode. In real seawater electrolytes, a mixed corrosion state occurs.

In summary, the presence of various halide ions in seawater, recognized for their corrosive and toxic properties, can significantly impact the stability of key components within an electrolyzer, including the anode and membranes. These impurities can compromise the stability of these components and reduce the stable service life of the anode. There are two main factors affecting anode stability: (1) severe corrosion of the electrode by chlorine-containing substances produced during electrolysis; (2) corrosion of the anode substrate. To achieve efficient seawater electrolysis, it is crucial to optimize the design of anode catalysts to regulate the catalytic reaction process, thereby mitigating the negative effects of these halide ions and enhancing the overall performance and longevity of the electrolysis system.

Focusing on the issue of chloride ions in seawater, the design principles for anode catalysts in direct seawater electrolysis include: (1) designing high-activity OER catalysts with lower overpotentials: by reducing the overpotential, the efficiency of the electrochemical reactions can be improved, thus minimizing the formation of harmful chlorine-containing species; (2) replacing OER with thermodynamically more favorable electro-oxidation reactions: this can potentially prevent the formation of corrosive chlorine species [26]; (3) constructing a Cl^- blocking layer at the electrode–electrolyte interface to inhibit the CER: this layer can prevent chloride ions from reaching the anode surface, thus reducing the corrosion risk [25,27,28]; (4) rapid in situ consumption of Cl^- or Cl_2 generated by CER: by quickly consuming these species, the corrosive impact can be minimized, protecting the anode from degradation.

3.1. Protection of Anode Current Collectors

Current collectors in electrocatalytic systems are critical components responsible for efficiently transmitting current to the catalyst's active surface, thereby enhancing overall system efficiency. They must exhibit exceptional conductivity, chemical stability, and corrosion resistance. Ideal materials, such as copper, silver, platinum, and carbon, should possess sufficient mechanical strength and surface roughness to reliably support catalyst loading. Structural designs featuring porous or mesh-like configurations increase contact area and reduce bubble accumulation, optimizing mass transfer and electrochemical performance.

In specialized applications like seawater electrolysis, where chloride and bromide ions in seawater continuously attack the anode under the influence of an electric field, current collectors must be able to withstand high salinity and corrosive substances. Otherwise, they risk severe corrosion. Surface modification and protective coatings can further enhance the durability and environmental adaptability of current collectors, thus ensuring the stability and cost-effectiveness of electrochemical systems over prolonged operation. The introduction of sulfides and phosphides into high-entropy alloys can change the electronic environment of metal active sites, thus enhancing the stability and activity of the catalysts for water electrolysis under electrochemical conditions, highlighting the potential of sulfides and phosphides for seawater splitting [29]. Currently, treatments such as sulfidation [25,30,31], phosphidation [32–34], selenization [35,36], and anion intercalation [37–39] are recognized as effective strategies for protecting the substrate of catalyst current collectors.

Kuang et al. developed a solvent-thermal treatment method on nickel foam [25], resulting in a uniform NiS_x layer formed on its surface through reactions with elemental sulfur in toluene. Subsequently, they deposited a NiFe-LDH nanosheet array catalyst on the NiS_x layer using electrodeposition technology, creating an innovative hierarchical multilayer electrode structure (Figure 2a). This structure not only endowed the electrode with excellent catalytic activity but also significantly enhanced its performance by forming a 1–2 μm thick NiS_x layer on the electrode surface (Figure 2b,c). Moreover, a vertically aligned NiFe-LDH nanosheet array layer successfully epitaxially grew on the NiS_x surface [40,41] (Figure 2d). Utilizing in situ generated poly-anions, a protective layer formed on the electrode surface that effectively resisted chloride ion corrosion in seawater. Furthermore, analysis using Time of Flight Secondary Ion Mass Spectrometry (TOF-SIMS) confirmed the insertion of sulfate and carbonate poly-anions, demonstrating the interlayer stability of the catalyst [42,43] (Figure 2e). Consequently, this electrode exhibited outstanding long-term stability in seawater electrolysis in high-concentration salt solutions. This study also found that after anodic activation in an alkaline simulated seawater electrolyte (1 M KOH + 0.5 M NaCl), the electrode displayed excellent catalytic activity, achieving an OER current density of 400 mA/cm^2 at a low overpotential of approximately 0.3 V. This low overpotential, well below 0.48 V, reduces the oxidation of chloride ions to hypochlorite salts in alkaline seawater.

Wang et al. delved deeply into the intrinsic connection between electronic structure and electrocatalytic activity during seawater electrolysis [44]. Through precise density functional theory (DFT) calculations, they discovered that introducing a phosphorus (P) vacancy can optimize the adsorption energy of intermediates [45], significantly enhancing the performance of electrocatalysts. The introduction of a P vacancy not only strengthened the adsorption energy of intermediates but also activated neighboring metal sites, imparting them with new electrocatalytic activity (Figure 2f). This strategy induces significant electron redistribution within the crystal, where P defects act as electron donors, adjusting the electron distribution in NiCoP, thereby promoting surface reconstruction processes to generate stable active sites and enhance the catalytic kinetics of OER [46].

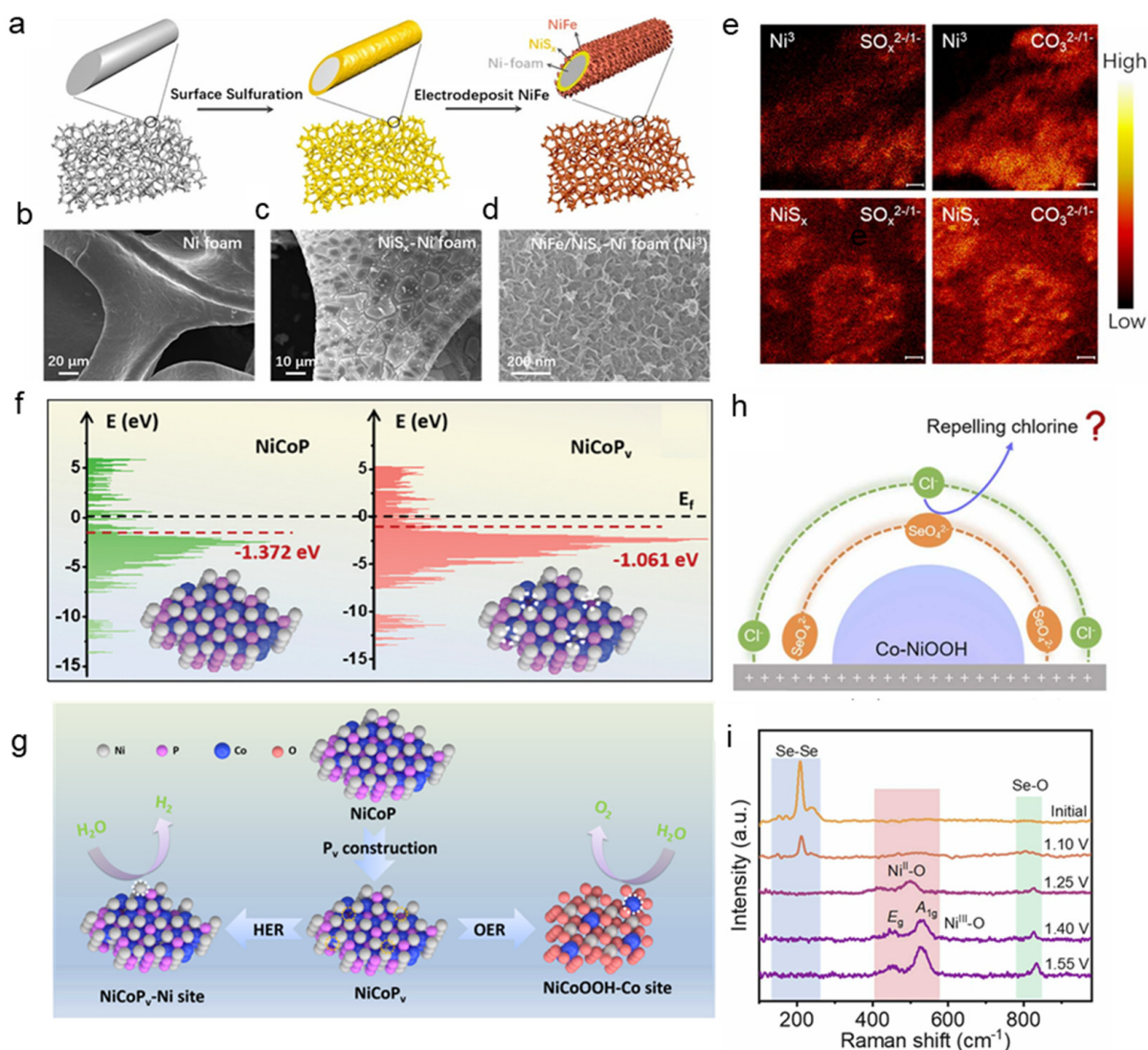


Figure 2. Protection of anode current collectors. (a) Schematic drawing of the fabrication process; (b–d) SEM images of untreated nickel foam, NiS_x formed on nickel foam, and electrodeposited NiFe on the NiS_x surface; (e) TOF-SIMS mapping of SO_x^{2-/1-} and CO₃^{2-/1-} fragments from a Ni₃ and NiS_x/Ni electrode surface after activation in 1 M KOH + 0.5 M NaCl at 400 mA/cm². Negative TOF-SIMS counts were collected from *m/z* = 96/48/80/40 (SO₄⁻/SO₄²⁻/SO₃⁻/SO₃²⁻) and 60/30 (CO₃⁻/CO₃²⁻) after Ar plasma milling for 5 to 15 min to clean the surface adsorbed electrolytes (scale bars: 10 μm); (f) The total DOS of NiCoP and NiCoP_v; (g) Schematic representation of the genuine phases and active sites of NiCoP_v in 1.0 M KOH + seawater electrolyte during HER and OER; (h) The schematic illustration of the reconstruction of Co-NiSe₂ to generate Co-NiOOH and SeO₄²⁻ SCL on the surface; (i) In situ Raman of Co-NiSe₂ under initial, 1.10, 1.25, 1.40, and 1.55 V.

Based on DFT-predicted theoretical foundations, the researchers employed a three-step strategy involving molten salt synthesis, thermal phosphorization, and immersion to successfully prepare NiCoP_v@NF nanosheet electrocatalysts on commercial nickel foam (NF). This electrocatalyst exhibited outstanding catalytic activity and stability in alkaline seawater solutions. Particularly noteworthy is that P defects effectively reduce the reconstruction energy barrier during the OER process, facilitating the local transformation into active NiCoOOH phases. During the electrocatalytic process, the Ni sites of NiCoP_v and the Co sites formed by phase transformation to NiCoOOH serve as active centers for the HER and OER processes, respectively (Figure 2g). Furthermore, the in situ-generated PO₄³⁻ on the electrode surface, through synergistic effects of electrostatic attraction and spatial

repulsion, effectively suppresses Cl^- corrosion in seawater, protecting the electrode from corrosion and further enhancing the durability of the electrocatalyst [44].

Cao et al. synthesized Co-NiSe₂ nanosphere catalysts via hydrothermal synthesis of a precursor of Co-Ni alkaline oxides, followed by calcination [36]. In situ experiments and theoretical studies confirmed that cobalt-doped nickel diselenide (Co-NiSe₂) facilitates rapid reconstruction into highly active cobalt-doped nickel oxyhydroxide (Co-NiOOH) by lowering the barriers for deselenization and dehydrogenation. This process also helps generate dynamically stable oxygen vacancy sites within the resulting Co-NiOOH, leading to high OER performance. Additionally, self-generated SeO₄²⁻ on the electrode surface selectively repels Cl^- without hindering the diffusion and adsorption of active species, thereby preventing the dissolution of metal species in Co-NiOOH (Figure 2h). In situ Raman spectroscopy further identified the active phases and dynamic reconstruction of Co-NiSe₂ (Figure 2i). For Co-NiSe₂, a distinct Raman band at 498.9 cm⁻¹, attributed to the Ni^{III}-O vibration of Ni(OH)₂, was detected. Under the corrected potential, a pair of peaks split at 451.6 and 526.4 cm⁻¹ corresponded to the E_g bending and A_{1g} stretching vibrations of Ni^{III}-O in NiOOH [7], respectively. Additionally, a new Se-O band associated with selenate (SeO₄²⁻) appeared at 828.2 cm⁻¹ at 1.25 V, with the Se-O band gradually intensifying as the potential increased, indicating the accumulation of more SeO₄²⁻ on the electrode surface due to the anodic charge and electric field [47].

These findings suggest that Co-NiSe₂ can quickly evolve into the active Co-NiOOH phase during reconstruction, accompanied by the formation of SeO₄²⁻ species on the electrode surface. This special treatment of the material surface enhances the stability and corrosion resistance of the catalyst in seawater, providing a new perspective for designing efficient and stable electrocatalysts. This approach opens new pathways for advancing the hydrogen economy.

3.2. Self-Reconstruction and Dynamic Dissolution of Catalyst

In environments containing chloride, such as direct seawater electrolysis, constructing a selective permeation barrier on the electrode–electrolyte interface can effectively limit the contact between Cl^- and the catalytic active sites of the electrode. Various electrodes, including nitrides, phosphides, sulfides, and selenides, undergo in situ surface transformations, producing negatively charged anionic layers upon oxidation [31,32,48,49]. These layers repel Cl^- and protect the anode from corrosion. This barrier acts as a protective shield, preventing anodic chlorination reactions that could generate chlorine gas or other harmful chlorides, leading to electrode corrosion or performance degradation. Consequently, this strategy not only avoids adverse side reactions but also significantly enhances the chemical stability and long-term durability of the electrode, which are crucial for improving the overall performance and reliability of electrochemical devices.

Liu et al. employed an innovative two-step synthesis strategy to successfully fabricate a cobalt ferricyanide/cobalt phosphide (CoFePBA/Co₂P) anode with a unique Cap/Pin structure [28] (Figure 3a). This structured electrode demonstrated exceptional performance during the electrolysis of saturated brine. Experimental data combined with molecular dynamics simulations revealed that during the oxygen evolution reaction (OER), the electrode surface undergoes reconstruction, forming a composite anionic layer of PO₄³⁻ and Fe(CN)₆³⁻. This novel anionic synergy mechanism provides significant protection for the electrode in real seawater environments by reducing Cl^- adsorption on the electrode surface through electrostatic repulsion and dense coverage, decreasing it by nearly fivefold. This results in excellent OER activity and prolonged electrolysis stability in high-concentration brine, making it suitable not only as a seawater electrolysis anode catalyst but also for brine lake electrolysis. This expands the application range of anode catalysts, offering new insights and solutions for seawater and brine lake water electrolysis.

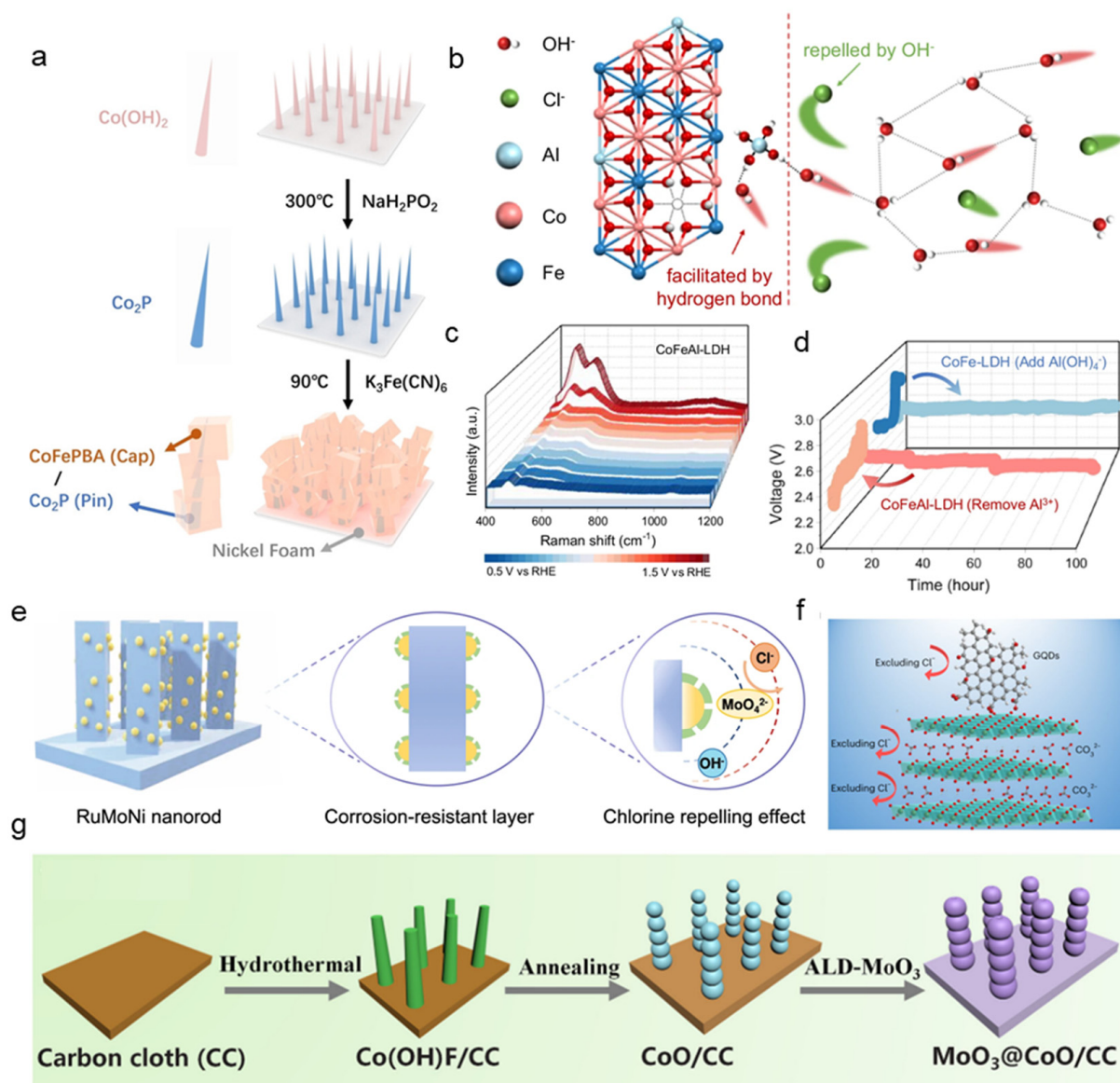


Figure 3. Self-reconstruction and dynamic dissolution of catalyst. (a) Schematic route for the synthesis of CoFePBA/Co₂P electrode; (b) Illustration of the corrosion resistance mechanism of surface adsorbed Al(OH)_n⁻; (c) Operando Raman spectrum of CoFeAl-LDH, potential range: OCP-1.5 V vs. RHE; (d) CP response at 0.2 Acm⁻² of CoFe-LDH before/after adding Al(OH)_n⁻ to the electrolyte, and CoFeAl-LDH before/after etching Al³⁺, in an electrolyte containing 20 wt.% NaOH + satu. NaCl; (e) A schematic showing the structure and corrosion-resistant strategy of the RuMoNi electrocatalyst. The light blue bar, yellow semicircle, and dotted green lines stand for nanorod-shape substrate, active sites, and corrosion-resistant layer, respectively; (f) Schematic illustration of CoFe-Ci@GQDs against Cl⁻ corrosion in seawater; (g) Schematic illustration of the synthesis process of MoO₃@CoO/CC.

In a subsequent study by the team, researchers ingeniously crafted a layered CoFeAl-LDH anode material, showcasing a unique self-protective mechanism during seawater oxidation reactions [27]. Specifically, under the erosive influence of OH⁻, aluminum (Al) gradually leaches out from the CoFeAl-LDH, creating abundant Al³⁺ vacancies. These vacancies not only enhance the catalytic activity of the OER but also spontaneously generate Al(OH)₄⁻ species due to the absence of Al³⁺ [50,51], which firmly adsorb onto the anode surface (Figure 3b), significantly enhancing the stability of seawater electrolysis processes. Through in situ Raman spectroscopy analysis, researchers observed a marked enhancement

in vibrational peaks associated with $\text{Al}(\text{OH})_n^-$ within the 400–700 cm^{-1} range, particularly a significant increase in signal intensity at the 988 cm^{-1} Al-O stretching vibration peak [52], further confirming the presence of $\text{Al}(\text{OH})_n^-$ on the electrode surface and its contribution to stability (Figure 3c).

To explore more deeply the specific role of $\text{Al}(\text{OH})_n^-$ in electrode stability, researchers conducted a control experiment: adding $\text{Al}(\text{OH})_n^-$ to the CoFe-LDH electrolyte. The results demonstrated a significant improvement in the stability of the CoFe-LDH electrode, with a voltage decay rate of only 0.29% during over 500 h of stability testing. This finding corresponds with the stability observed in CoFeAl-LDH after the formation of Al^{3+} vacancies and $\text{Al}(\text{OH})_n^-$. Conversely, removing the $\text{Al}(\text{OH})_n^-$ from CoFeAl-LDH resulted in a sharp decline in electrode stability, with a voltage decay rate reaching 16.41% within just 10 h of testing (Figure 3d). This controlled experiment strongly validates the crucial role of $\text{Al}(\text{OH})_n^-$ in enhancing electrode stability, revealing its potential application value for seawater electrolysis. Through this material design, CoFeAl-LDH achieves not only efficient OER catalytic performance but also demonstrates excellent corrosion resistance, thus offering new avenues and strategies for the advancement of seawater electrolysis technology.

Kang et al. successfully synthesized a novel RuMoNi catalyst through a two-step synthesis strategy [53]. Initially, a hydrothermal synthesis method was employed, followed by electrochemical activation to obtain the catalyst with a unique structure. This catalyst consists of a Ni_4Mo nanorod substrate, uniformly anchored with RuO_2 particles and covered by a layer of NiMoO_4 , forming a composite nanostructure (Figure 3e). During the electrochemical oxidation process, Inductively Coupled Plasma Optical Emission Spectroscopy (ICP-OES) detected that the concentration of Mo atoms in the electrolyte remained constant. This phenomenon is likely due to the dynamic dissolution and precipitation reactions of NiMoO_4 and MoO_4^{2-} at the electrochemical interface, thereby maintaining the stability of MoO_4^{2-} concentration in the electrolyte. During electrolysis, the multivalent MoO_4^{2-} anions preferentially adsorb onto the electrode surface owing to electrostatic attraction [54]. This adsorption not only effectively blocks Cl^- through electrostatic repulsion but also enhances the corrosion resistance of the electrocatalyst [25,55,56]. Simultaneously, the strong hydrogen bonding between the Ni_4Mo surface and OH^- facilitates the approach and participation of OH^- in the reaction, effectively alleviating the adverse effects of electrostatic repulsion on OH^- and maintaining rapid oxygen evolution reaction (OER) kinetics [7].

In their groundbreaking study, Zou et al. anchored graphene quantum dots (GQDs) onto the surface of the CoFe-LDH catalyst and simultaneously introduced carbonate ions (CO_3^{2-}) into its interlayer structure [37] (Figure 3f). This innovative dual strategy not only significantly enhances both the stability and efficiency of the catalyst but also establishes an effective protective mechanism against the corrosive effects of chloride ions in complex seawater environments.

Firstly, anchoring graphene quantum dots (GQDs) onto the catalyst surface represents a novel approach that stabilizes the active sites through their electron-donating effects. The negative charge characteristics of GQDs help prevent adverse adsorption of Cl^- at the active sites, thereby protecting the catalyst from corrosion by high concentrations of Cl^- in seawater. This surface-modification strategy not only enhances the corrosion resistance of the catalyst but also facilitates the dissociation of water molecules and proton-electron coupled transfer processes, crucial for improving the efficiency of the oxygen evolution reaction (OER). Secondly, the introduction of CO_3^{2-} represents another innovative step, establishing strong repulsive forces within the interlayers of CoFe-LDH that effectively resist Cl^- intrusion. Due to their small size and high negative charge density, CO_3^{2-} forms strong electrostatic interactions with the main layers of CoFe-LDH, significantly enhancing the stability of the interlayer structure and greatly improving its ability to repel chloride ions, thereby inhibiting the collapse of the layered structure and catalyst corrosion.

Guo and his team synthesized a $\text{Co}(\text{OH})_2$ precursor on a carbon cloth substrate using a hydrothermal method, which was then transformed into a bead-like CoO structure through

a precisely controlled annealing process [57] (Figure 3 g). This procedure laid the foundation for the subsequent atomic layer deposition (ALD) technique [58,59], which facilitated the uniform deposition of an ultrathin amorphous MoO_3 layer on the CoO surface, resulting in the innovative $\text{MoO}_3@ \text{CoO}/ \text{CC}$ catalyst structure. The pea-like $\text{MoO}_3@ \text{CoO}/ \text{CC}$ catalyst demonstrated excellent catalytic performance.

After activation, the $\text{MoO}_3@ \text{CoO}/ \text{CC}$ catalyst maintained its pea-like morphology, but significant interface changes between the MoO_3 layer and the CoO substrate were observed. Specifically, darker regions appeared between the two phases, and the interlayer spacing increased significantly, indicating the formation of a new stable phase at the interface. High-resolution transmission electron microscopy (HR-TEM) analysis confirmed that the lattice spacing was 0.38 nm, corresponding to the (006) plane of CoMo-LDH [60]. This finding demonstrates that the material underwent a constrained dynamic surface self-reconstruction mechanism during activation, forming a CoMo-LDH layered structure with strong electrostatic repulsion against Cl^- .

Moreover, the MoO_3 layer acted as a directional confinement layer, regulating the formation of CoMo-LDH, and optimized the catalytic activity sites through refined interface engineering, enhancing the catalytic reaction kinetics. The researchers explored the electrode behaviors of self-leaching and dynamic dissolution, providing new insights into designing high-performance seawater electrolysis and salt-resistant catalysts.

3.3. Regulation of the Surface Microenvironment and Ligand Regulation

The formation of a negatively charged anionic layer on the catalyst surface during oxidation effectively repels Cl^- ions and shields the anode from corrosion, serving as a robust anti-corrosion strategy. Furthermore, researchers have successfully mitigated the attack of chloride ions (Cl^-) on the anode catalyst by regulating the atomic coordination of the catalyst and optimizing the surface microenvironment [58].

Sha et al. presented a pioneering study proposing a unique strategy to significantly enhance the catalytic performance of the oxygen evolution reaction (OER) by modulating the adsorption behavior of chlorine ions (Cl^-) on monatomic iridium (Ir) catalysts. Unlike previous catalysts designed to repel Cl^- adsorption, the Ir/CoFe-LDH catalysts in this study utilize atomically dispersed Ir sites to allow Cl^- adsorption, modulating the electronic structure of the Ir active center and forming a unique Ir-OH/Cl coordination state [60]. When NaCl was added to the 6 M of NaOH electrolyte to simulate a seawater environment, the OER overpotential of Ir/CoFe-LDH was reduced from 236 mV to 202 mV, and the TOF (rate of oxygen generation per second) significantly increased. This indicates that the OER performance of the catalyst is significantly enhanced at a specific $\text{Cl}^- / \text{OH}^-$ ratio. Studying different $\text{Cl}^- / \text{OH}^-$ ratios helps determine the optimal operating conditions for the catalyst under actual seawater electrolysis conditions. As shown in Figure 4a, the OER overpotential of Ir/CoFe-LDH at a current density of 10 mA cm^{-2} initially decreased and then increased with rising Cl^- concentration when the NaOH concentration increased from 1 M to 6 M. The optimal OER performance of Ir/CoFe-LDH was observed at a $\text{Cl}^- / \text{OH}^-$ ratio of 1:2, highlighting the critical influence of chloride ions on OER performance. The TOF value of Ir/CoFe-LDH in 6 M NaOH + 2.8 M NaCl electrolyte ($7.46 \text{ O}_2 \text{ s}^{-1}$) was 7.1 times higher than in 6 M of NaOH electrolyte ($1.05 \text{ O}_2 \text{ s}^{-1}$) at 1.5 V vs. RHE. Additionally, the catalyst remained stable for over 1000 h at industrially relevant current densities ($0.4\text{--}0.8 \text{ A cm}^{-2}$) and for over 2000 h in real seawater.

In situ Raman spectroscopy was employed in this study to investigate the effect of chloride ions on the oxygen evolution reaction (OER) activity when adsorbed on iridium monatomic catalysts. Through in situ Raman spectroscopy, researchers observed a new peak in the Raman spectrum of Ir/CoFe-LDH at nearly 333 cm^{-1} under open-circuit voltage (OCV) conditions, attributed to the vibrational mode of Ir-Cl. This indicates the formation of Ir-Cl coordination at the Ir monatomic site (Figure 4b). In NaOH and NaOH + NaCl electrolytes, the Ir-Cl coordination peak at 333 cm^{-1} persisted. However, in alkaline electrolytes without Cl^- , Ir-Cl coordination was observed only under open-

circuit voltage conditions and disappeared when voltage was applied. This suggests significant competition between Cl^- and OH^- for adsorption onto Ir monatomic sites at high OH^- concentrations, indicating that higher NaCl concentrations are required to maintain the stability of Ir-Cl coordination.

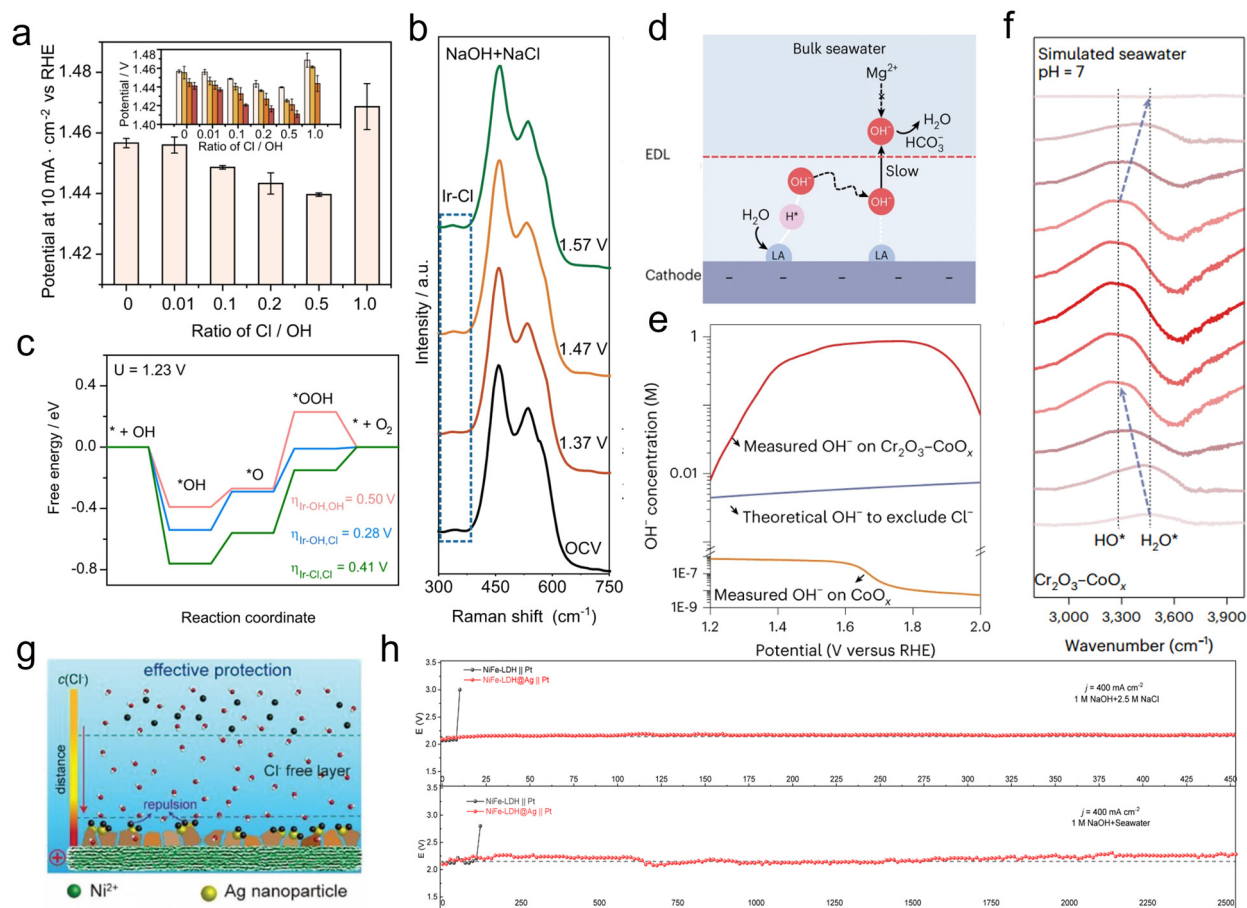


Figure 4. Regulation of the surface microenvironment and ligand regulation. (a) Comparison of OER overpotential at a current density of 10 mA cm⁻² of Ir/CoFe-LDH in electrolyte with different Cl⁻/OH⁻ ratios in 1 M of NaOH. The inset shows the OER overpotential of Ir/CoFe-LDH at a current density of 10 mA cm⁻² with different Cl⁻/OH⁻ ratios in 1 M (white), 2 M (yellow), 3 M (orange), and 6 M of NaOH (red). (b) In situ Raman spectra of Ir/CoFe-LDH recorded in NaOH+NaCl. (c) The activation energy of Ir/CoFe-LDH with three coordination states. (d) Schematic diagram of local alkaline microenvironment generation on Lewis acid-modified cathode, which facilitates HER and prevents precipitate formation. (e) Measured OH⁻ concentration and theoretical concentration of excess OH⁻ required to resist Cl⁻ (f) show that on Cr₂O₃-CoO_x, the H₂O* band shifts continuously toward the OH* band when the anodic potential increases. It is important to note that the spectra were plotted using the curve measured at 0.90 V vs. RHE as a baseline. (g) Schematic illustration of the effect of the SCI strategy on the prevention of corrosion by chloride ions. (h) Durability tests of NiFe-LDH and NiFe-LDH@Ag anodes, paired with a Pt cathode, at a constant current density of 400 mA cm⁻² in different electrolytes (1 M NaOH + 2.5 M NaCl, 1 M NaOH + seawater).

Introducing chloride ions (Cl⁻) revealed that dynamic adsorption on the iridium (Ir) site not only lowered the activation energy barrier for the oxygen evolution reaction (OER) but also enhanced the adsorption of *OOH intermediates through the formation of Ir-OH/Cl coordination, which is crucial for the OER rate-determining step (Figure 4c). This strategy effectively inhibits the competitive CER by forming stable Ir-Cl bonds on Ir atoms, providing additional structural stability that reduces solvation or structural changes of CoFe-LDH during electrochemical oxidation [61,62]. Furthermore, this bonding

modulates the electronic structure of CoFe-LDH by redistributing electrons, improving its structural integrity and functionality in an electrochemical oxidation environment. The catalytic selectivity and stability were maintained close to 100%. Experimental and theoretical calculations demonstrated that the Ir/CoFe-LDH catalyst exhibited excellent OER activity under alkaline seawater electrolysis conditions. Specifically, Ir/CoFe-LDH showed exceptional oxygen evolution reaction activity in 6 M NaOH + 2.8 M NaCl, with an overpotential of only 202 mV at a current density of 10 mA cm^{-2} , which is 34 mV lower than in 6 M of NaOH electrolyte (236 mV). This significant reduction in overpotential indicates the enhancement of OER activity by chloride ions.

This study not only delivers an efficient anode catalyst for seawater electrolysis but also presents a novel method to modulate single-atom catalysts for catalytic reactions in diverse neutral environments. The researchers effectively utilized the abundant Cl^- resource in seawater to enhance catalytic performance, thereby paving a new path toward achieving efficient and stable hydrogen production via seawater electrolysis.

As shown in Figure 4d, Qiao et al. proposed an innovative strategy to significantly enhance seawater electrolysis performance by introducing a Lewis acid layer on the catalyst surface. The core of this approach involves using hard Lewis acids (e.g., Cr_2O_3) to interact with water molecules, dynamically splitting them and trapping the hydroxyl anions (OH^-), thereby generating a localized alkaline environment in situ. This facilitates the kinetics of the electrode reaction while inhibiting the harmful effects of chloride ions and preventing the formation of precipitates.

The proposed Lewis acid layer effectively traps and enriches hydroxyl anions and modulates the charge and pH on the catalyst surface, providing more favorable conditions for the adsorption and dissociation of water molecules [63]. Since OH^- and Cl^- are the primary anions in seawater, the accumulation of excess OH^- on the anode surface reduces the amount of Cl^- . This occurs because OH^- and Cl^- compete for adsorption sites on the electrode surface, with more OH^- preventing Cl^- from approaching the electrode surface. Using the IrO_x -modified rotating ring disk electrode technique, the authors found that the pH of the Cr_2O_3 - CoO_x surface increased with applied potential, then initially increased and subsequently decreased with current density. In contrast, the pH of the CoO_x surface was lower than seawater (~7.9) and decreased with increasing current density (Figure 4e). Even at anodic potentials as high as 1.90 V vs. RHE, the OH^- concentration on the Cr_2O_3 - CoO_x surface remained significantly higher than the theoretically required excess OH^- concentration, suggesting that the OH^- generated on the surface of Cr_2O_3 - CoO_x is sufficient to inhibit the migration of Cl^- from seawater to the electrode surface [64,65]. These results clearly demonstrate the Cr_2O_3 layer's ability to successfully generate localized alkalinity on the catalyst surface. The article used in situ surface-enhanced infrared reflectance (IR) spectroscopy to probe the formation mechanism of locally generated OH^- on the anode surface in natural seawater. For CoO_x , the band at 3460 cm^{-1} was assigned to adsorbed water molecules (H_2O^*), which did not shift significantly with varying applied voltage. However, for Cr_2O_3 - CoO_x , the H_2O band continued to shift toward the OH band when the applied potential varied from 1.0 V vs. RHE to 1.8 V vs. RHE (Figure 4f), suggesting that the localized OH^- generated arises from the dissociation of adsorbed water molecules on Cr_2O_3 [66–68].

Using density-functional theory (DFT) calculations and in situ infrared spectroscopy, the researchers revealed how the Lewis acid layer facilitates the decomposition of water molecules to generate key active intermediates. Additionally, experimental results show that the performance of this surface-modified catalyst in natural seawater is comparable to that of a proton-exchange membrane (PEM) electrolyzer in high-purity water, achieving long-term stable performance for over 100 h at a current density of 500 mA cm^{-2} . This study optimizes the seawater-electrolysis process through fine-tuning of surface chemistry. This approach not only improves electrolysis efficiency but also enhances system stability, opening new avenues for efficient and economical hydrogen production from seawater electrolysis.

Lu et al. proposed an innovative strategy to immobilize chloride ions by loading silver (Ag) nanoparticles onto the surface of the catalyst, significantly improving the stability of the anode in seawater electrolysis (Figure 4g). The core of this strategy involves using silver nanoparticles to react with free chloride ions (Cl^-) in seawater, forming stable silver chloride (AgCl) under an applied electric field, thereby creating a protective layer on the anode surface. Specifically, an optimized nickel-iron layered double hydroxide (NiFe-LDH) was used as a catalyst in the study, and Ag nanoparticles were loaded onto it by electrodeposition to prepare the NiFe-LDH@Ag electrode [69]. The experimental results showed that the stability of this modified electrode in 1 M NaOH + 2.5 M NaCl or 1 M NaOH + seawater electrolyte reached over 450 h and 2500 h, respectively, which far exceeded the stability of the unmodified NiFe-LDH electrode (Figure 4h).

Through various analytical techniques, the researchers found that Ag nanoparticles are converted to AgCl during oxidation instead of Ag_2O in conventional alkaline electrolytic water. AgCl has a solubility product (K_{sp}) of 1.8×10^{-10} , making it virtually insoluble in water. The formation of this AgCl layer produces two main effects on the anode surface to resist Cl^- : the first is a physical barrier. The AgCl layer, as an insoluble layer covering the anode surface, provides a physical barrier for the anode, preventing direct contact between Cl^- and the anode material, thus reducing the occurrence of corrosion reactions. Co-ionic effect: after the formation of the AgCl layer, since Cl^- has been immobilized in AgCl, this creates a high concentration of Cl^- in the local area. According to Le Chatelier's principle, this inhibits more Cl^- from approaching the anode surface because there is already enough Cl^- in the system to combine with Ag^+ to form AgCl.

This co-ionic effect leads to a reduction in the concentration of Cl^- in the vicinity of the anode, further slowing the corrosion process. Through molecular dynamics simulations and experimental measurements of the capacitance of electrochemical double layers (CEDL) [47], the researchers observed almost no free Cl^- present on the AgCl surface, confirming the effectiveness of the AgCl layer in inhibiting Cl^- corrosion. Thus, the formation of AgCl significantly reduces the concentration of free Cl^- ions near the anode surface, effectively inhibiting the corrosive effect of Cl^- ions on the anode.

3.4. Design of Seawater Electrolysis Electrolyzer

The indirect decomposition of seawater through pre-desalination avoids side reactions and corrosion issues but requires additional energy input, reducing its economic viability. In contrast, integrating in situ seawater purification technology into an electrolyzer simplifies the process and reduces the footprint, making it highly appealing compared to step-by-step seawater purification–electrolysis systems [70,71]. Xie et al. proposed an innovative electrolyzer design (Figure 5a) specifically tailored for direct seawater electrolysis to produce hydrogen. This design employs a phase change-migration mechanism based on water vapor pressure differentials, facilitating spontaneous water migration from seawater to the electrolyte side. It utilizes a hydrophobic porous polytetrafluoroethylene (PTFE) membrane as the gas-phase interface and a concentrated potassium hydroxide (KOH) solution as the self-suppressing electrolyte, effectively preventing liquid seawater and ionic contaminants from penetrating [8].

The main advantage of this design is its 100 percent ion-blocking efficiency, which ensures that the “pure water” used in the electrolysis process comes directly from seawater, eliminating the need for an additional desalination step. This is crucial for reducing hydrogen production costs and improving energy efficiency. Additionally, since the water-migration process is spontaneous, no additional energy input is required, further reducing the overall energy consumption of the system. In terms of performance and reliability, the reported electrolyzer has demonstrated excellent long-term stability under real-world application conditions, operating stably at a current density of 250 mA cm^{-2} for over 3200 h without maintenance. During the electrolysis process, the relative Faraday efficiency (RFE) for oxygen was close to 100 percent, and no chlorine (Cl_2) generation was detected, indicating that the electrolysis process is highly selective and capable of efficiently converting

seawater into hydrogen and oxygen without generating harmful by-products. In terms of energy consumption, the electrolyzer's energy use is comparable to that of industrial alkaline water electrolysis, with production costs of approximately 4.6 kWh and 5.3 kWh per standard cubic meter of hydrogen at current densities of 250 mA cm⁻² and 400 mA cm⁻², respectively. This level of energy consumption is economically viable for large-scale hydrogen production and competitive with current industrial water electrolysis technologies.

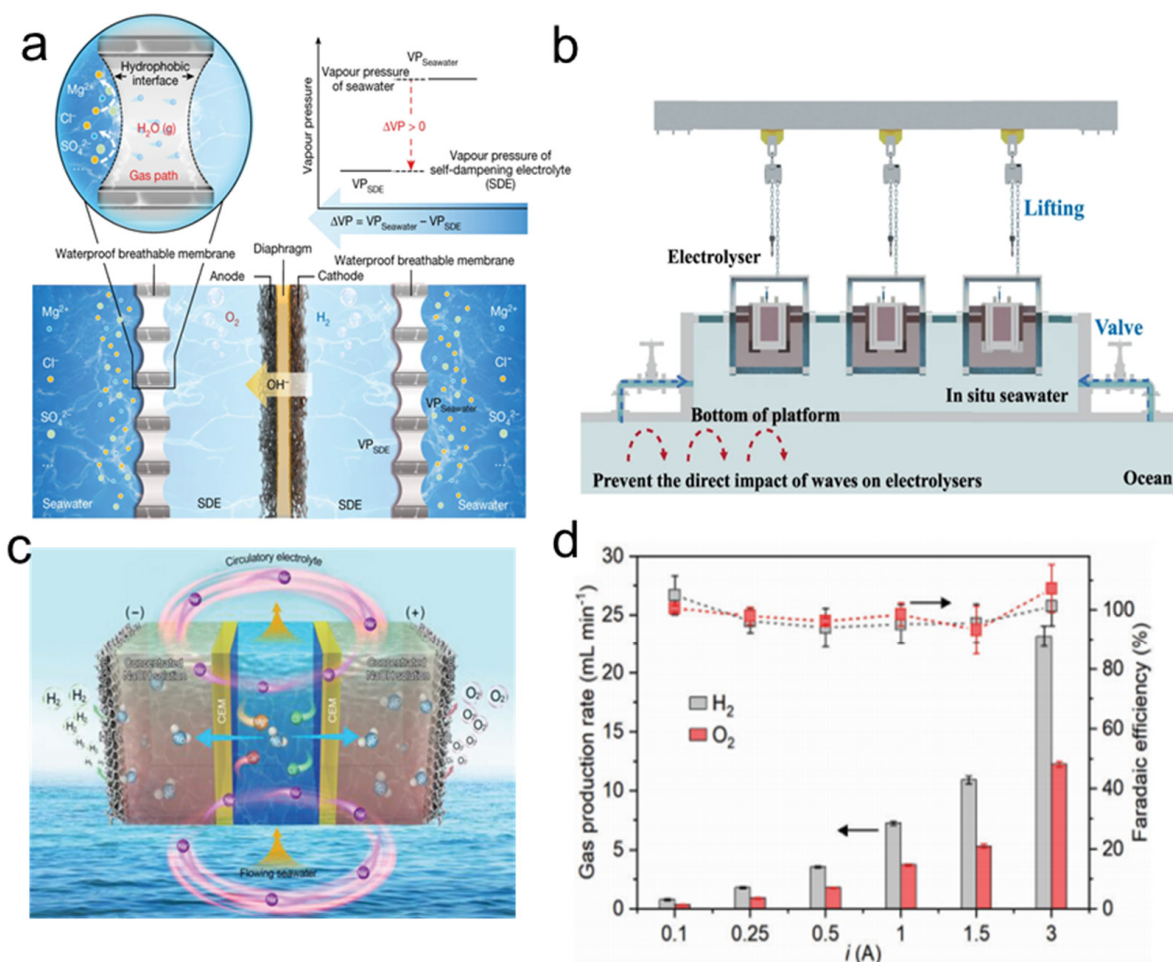


Figure 5. Design of seawater electrolysis electrolyzer. (a) The liquid gas–liquid phase transition-based migration mechanism of the water purification and migration process and the driving force. (b) Diagram of the seawater cabin connected to the ocean. (c) Schematic of the continuous direct seawater electrolysis (DSE) system based on a dual-CEM three-compartment architecture integrated with a circulatory electrolyte design. HER and OER take place at cathode and anode in the circulating NaOH electrolyte, respectively. (d) HER/OER Faradaic efficiency and the gas production rates of the direct seawater electrolysis (DSE) systems determined using galvanostatic electrolysis.

Furthermore, based on this electrolyzer design, the researchers further explored its feasibility and performance in large-scale applications. The research team demonstrated a kilowatt-scale floating electrolysis platform in practical operation in Xinghua Bay, integrating energy storage, current conversion, hydrogen detection, and transport modules [3]. This system utilizes offshore wind energy as a power source and ensures the continuity and stability of the electrolysis process through the floating platform's stability and energy-management system (Figure 5b). Hydrogen production at a scale of 1.2 Nm³ h⁻¹ was successfully realized. This achievement demonstrates the technology's applicability and stability in real marine environments. This study also considered the effects of the fluctuating marine environment on the water-migration and electrolysis processes. Laboratory simulations and at-sea tests showed that the fluctuating environment actually

facilitated water mass transfer and that the stability of core components (e.g., membranes or catalysts) was not significantly affected. This is because the fluctuations increase the surface area of seawater in contact with the PTFE membrane, thus increasing the amount of water migration per unit of time. Additionally, the movement of seawater counteracts the transient increase in brine concentration at the membrane surface, further facilitating water migration. This finding is critical to understanding and optimizing the performance of electrolyzers in dynamic marine environments. Furthermore, the research identifies technical challenges for key system components and examines the long-term stability and ion-blocking efficiency of electrolyzers under complex and changing ocean conditions. These studies provided scientists with a deeper understanding of how to improve the economic viability of on-site direct seawater electrolysis based on renewable energy inputs.

At the forefront of green hydrogen energy production, Ren et al. pioneered groundbreaking research by designing and demonstrating an innovative electrolyzer featuring a “triple-chamber, double-positive membrane, and recirculating electrolyte” structure (Figure 5c). This configuration provides a highly efficient solution for continuous hydrogen production from seawater. The core innovation of their research lies in a novel electrolysis system that effectively addresses challenges such as ionic interference and chlorine corrosion, typically associated with conventional seawater electrolysis, thereby paving the way for a new approach to clean energy production [72].

The electrolyzer’s three-chamber design, with a central seawater chamber and electrolyte chambers on both sides, ensures orderly migration of water molecules and precise ion screening through a monovalent ion-selective cation exchange membrane. The experiments investigated water mobility through the cation-exchange membrane and established the relationship between water mobility and the concentration gradient on both sides of the membrane. According to Fick’s law, water mobility is proportional to the surface area and the concentration gradient on both sides of the membrane [73]. Adjusting the concentration gradient on both sides of the membrane allows for achieving a dynamic water equilibrium in a continuous direct water electrolysis system. This structure ensures ion neutrality during electrolysis and maintains a constant concentration gradient and pH through a self-circulating electrolyte design, providing a continuous driving force for water molecule migration. The electrolyzer operates based on an electrochemical process, enabling efficient energy conversion through the HER and OER at the cathode and anode, respectively. The continuous direct seawater electrolysis (DSE) system, using natural seawater as the water source, operates stably over a current range of 0.1 to 3.0 A, with the rate of hydrogen and oxygen production increasing with current while maintaining a Faraday efficiency close to 100% [74] (Figure 5d). Energy consumption was evaluated by measuring electrical energy consumption during the electrolysis process, directly relating to the economics of the electrolyzer and its potential for large-scale applications. This design can produce hydrogen from flowing seawater at a rate of 7.5 mL/min for more than 100 h at an industrially relevant current of 1.0 A.

As shown in Table 1, indirect seawater-electrolysis technologies frequently integrate advanced desalination methods, such as reverse osmosis, with proton-exchange membrane (PEM) electrolysis. This integration minimizes interference from solid particles, microorganisms, and impurity ions. However, the pre-treatment phase can be energy-intensive, resulting in high energy consumption, a significant equipment footprint, and increased overall costs. In situ desalination electrolysis effectively combines membrane-separation technology with the electrolysis of purified water. However, the production capacity of these devices is limited by the membrane’s flux. Proton-exchange membrane water-electrolysis technology offers advantages such as low energy consumption, even under fluctuating conditions. However, it typically utilizes noble metal-based catalysts, which are costly, and operates in an acidic electrolyte that can be highly corrosive to the electrolyzer electrodes. Alkaline water electrolysis typically employs non-noble metal-based catalysts, thereby reducing costs. Nonetheless, it is characterized by a slow start-up time and poses potential safety risks due to hydrogen gas permeation. Direct seawater

electrolysis avoids competition for freshwater resources that are essential for human survival. Nevertheless, as mentioned above, it presents challenges such as anode corrosion and cathode precipitation, which require more effective solutions to advance seawater electrolysis toward industrialization.

Table 1. Comparison of hydrogen production routes from electrolytic water.

Technical Routes	Advantage	Disadvantage	Water Source
Indirect seawater electrolysis	High technical maturity [75]	Desalination equipment covers a large area	Ultrapure water
Direct seawater electrolysis	Coupled renewable energy, saving fresh water [75]	Anodic corrosion; cathode precipitation problem	Seawater
In situ desalination and electrolysis of seawater	Integrated membrane separation technology with water electrolysis [8]	Equipment size restricted by membrane flux	Seawater
Proton-exchange membrane water electrolysis	Anti-fluctuation, low energy consumption, fast start and stop [76]	Precious metal-based catalyst, electrode plate is easily corroded	Fresh water
Alkaline water electrolysis	Low cost by using non-precious metal based catalysts [76]	High energy consumption, slow start and stop, easy for hydrogen penetration and other problems to occur	Alkaline fresh water

4. Summary and Outlook

The success of direct seawater electrolysis (DSE) technology, an advanced method for producing green hydrogen, depends critically on the design and development of efficient catalysts. Researchers are currently focusing on developing electrocatalysts capable of maintaining high activity, selectivity, and stability in the complex medium of seawater. These catalysts must efficiently promote the OER and HER in near-neutral or alkaline seawater environments while inhibiting unfavorable side reactions such as the CER [77]. Researchers have employed various strategies to enhance catalyst performance, including innovative catalyst design, self-cleaning cathodes to prevent precipitation, the protection of anode current collectors, self-reconstruction and dynamic dissolution of anode catalysts, surface microenvironment regulation, and coordination modulation to resist seawater corrosion. Nonetheless, numerous challenges remain in the field of seawater electrolysis.

Firstly, in the complex environment of seawater electrolysis, cathode design must balance hydrogen evolution performance with anti-precipitation capability. Tang's team maintained the pH stability of the electrode surface and removed precipitates from the electrode surface by utilizing the external flow field generated by bubble desorption [18]. Although this strategy has been successful on a laboratory scale, the high current densities in industrial electrolysis require addressing the bubble shielding effect and the increased ohmic overpotential. At the industrial scale, the impact of bubbles on the catalyst is more significant, necessitating a deeper understanding of bubble behavior [78]. To achieve efficient electrolysis at an industrial scale, research on bubble behavior must be strengthened, and electrode design must be optimized for mass transfer and flow field distribution under industrial conditions [79]. Through these measures, electrolysis efficiency can be improved, energy consumption reduced, and the development of seawater electrolysis technology promoted to support greater efficiency and environmental friendliness.

Secondly, the mechanisms of catalyst degradation caused by various soluble ions in natural seawater remain unclear. Although catalyst engineering using polyanion coatings to inhibit chloride ion corrosion or to fabricate highly selective electrocatalysts has seen some success, it remains unsatisfactory in practical applications. Currently, poor anode stability due to the high Cl^- concentration in seawater is widely regarded as the main bottleneck restricting the development of this technology. Consequently, various anodes with high efficiency against Cl^- corrosion and enhanced stability have been developed. However, the stability of these anodes tested in alkaline seawater electrolysis for hydrogen production is significantly shorter than in alkaline simulated seawater (0.5 M NaCl). Therefore, it is crucial to investigate the detrimental effects of other chemical components in seawater

on anode stability to enhance anode lifetime and achieve industrial-scale application of seawater electrolysis. For example, besides Cl^- , Br^- in seawater is more detrimental to nickel-based anodes. Xu et al. found that the corrosion resistance of nickel substrates in Br^- -containing solutions was poorer than in Cl^- -containing solutions, and the corrosion rate in Br^- -containing solutions was faster, as shown by cyclic polarization curves [4]. Further electrochemical in situ characterization revealed that Cl^- causes localized corrosion of the substrate with narrow and deep pits, whereas Br^- corrodes over a large area with shallow and wide pits. Therefore, an in-depth understanding of the mechanisms by which soluble ions and other impurities in seawater cause catalyst degradation is essential for improving catalyst and electrode activity, extending the service life of electrolyzers, and reducing operation and maintenance costs.

Furthermore, current research tends to focus on catalyst development while neglecting their application in specific electrolyzer devices. Studies on electrolyzer technology often lack comprehensiveness and do not cover all possible configurations, resulting in unsatisfactory practical performance at the plant level. In rationalizing catalyst design for direct seawater electrolysis, it is crucial to consider the unique requirements of different electrolysis units and to take effective measures to address specific issues, thereby overcoming critical bottlenecks in both catalyst and unit design.

Hydrogen production by alkaline seawater electrolysis is considered a promising future technology for green hydrogen production due to its advantages of eliminating the need for a complex desalination process, suppressing chlorine precipitation side reactions, and fully utilizing excess renewable energy sources at sea promptly. For alkaline seawater electrolysis equipment, only the catalyst requires modification and design for industrial application. However, the current density cannot yet reach $0.8\text{--}1\text{ A/cm}^2$. Future alkaline seawater electrolysis equipment needs to increase the current density while reducing anode overpotential, improve anode catalyst selectivity under high currents, and reduce energy consumption under a high current density. Additionally, alkaline seawater electrolysis is less resistant to fluctuations, with the main problem being high hydrogen leakage in the partial load range, which leads to shutdown when hydrogen seepage in oxygen reaches 2 vol.% [80,81]. Therefore, the electrolyzer needs to be operated during periods of sufficient renewable energy supply. The fluctuating nature of renewable energy amplifies electrode degradation, a problem that must be addressed by developing stable electrode catalysts [82,83]. Compared to alkaline seawater electrolyzers, alkaline membrane seawater electrolyzers have the advantages of compactness, low hydrogen permeability, resistance to fluctuations, and low energy consumption [84]. However, alkaline membrane seawater electrolysis equipment is still in the research phase. Maintaining local pH stability in seawater, solving anode selectivity and cathode hydroxide deposition issues, and vigorously developing anion-exchange membranes are the primary directions for its future development.

The in situ desalination plant holds high potential for application as it achieves direct electrolysis for in situ desalination of seawater without increasing operating costs or footprint. However, its current capacity is small, and future development will require expanding the water flux and integrating with megawatt-scale equipment. The main challenge faced by acid membrane seawater electrolysis plants is the anodic chlorine oxidation competition reaction; hence, the feasibility of cathodic feed should be considered to minimize the interaction between chloride ions and the anode. Solid oxide electrolyzers can produce clean vapor before seawater reaches the catalyst, avoiding the detrimental effects of seawater impurities on the electrolyzer. However, their higher operating temperatures can affect the long-term operational stability of the electrolyzer components. Therefore, scaling up and selecting high-temperature-stable electrolyzer components are the focus of future development. New types of electrolyzers, such as bipolar membrane electrolyzers, have shown strong innovative potential; however, compared to the aforementioned technological routes, they are still some times away from large-scale industrial application.

Overall, seawater electrolysis for hydrogen production holds significant potential for application and development. Through continuous technological innovation and engineering optimization, seawater electrolysis for hydrogen production is expected to become the primary method for green hydrogen production in the future, significantly contributing to global energy transition and environmental protection goals.

Author Contributions: Writing—original draft, Y.Z. (Yixin Zhang) and Y.Z. (Yu Zhang); writing—review and editing, Q.S., Y.K. and C.W.; formal analysis, Q.S. and Z.L. (Zhichuan Li); investigation, E.Y. and H.Y.; validation, X.G. and Z.L. (Zihang Li); resources, Y.K. and Q.S.; project administration, Y.K. and D.Z.; funding acquisition, Y.K. and D.Z. All authors have read and agreed to the published version of the manuscript.

Funding: This work was supported by Science and Technology Innovation Foundation of Laoshan Laboratory (No. LSKJ202205700), Shenzhen Science and Technology Program (JCYJ20230807151159002), the Xinjiang Uygur Autonomous Region Key R&D Projects (No. 202114958), and the Cnooc Energy Technology & Service Limited, Clean Energy Branch. The authors also thank for National Key R&D Program of China (2021YFA1502200), the National Natural Science Foundation of China, and the Key Research Project of the Beijing Natural Science Foundation. D.Z. acknowledges financial support from the Young Elite Scientists Sponsorship Program by CAST (2022QNRC001).

Data Availability Statement: The data that support the findings of this study have been included in the main text. All other relevant data supporting the findings of this study are available from the corresponding authors upon request.

Conflicts of Interest: The authors declare that this study received funding from Cnooc Energy Technology & Service Limited, Clean Energy Branch. The funder was not involved in the study design, collection, analysis, interpretation of data, the writing of this article, or the decision to submit it for publication.

Abbreviations

LDH	Layered double hydroxide.
OER	Oxygen evolution reaction.
HER	Hydrogen evolution reaction.
CER	Chlorine evolution reaction.
MBPTS	Microscopic bubble/precipitate traffic system.
TOF-SIMS	Time of flight secondary ion mass spectrometry.
DFT	Density functional theory.
NF	Nickel foam.
GQDs	Graphene quantum dots.
OCV	Open-circuit voltage.
PEM	Proton-exchange membrane.
CEDL	Capacitance of electrochemical double layers.
DSE	Direct seawater electrolysis.
PTFE	Porous polytetrafluoroethylene.
SDE	Self-suppressing electrolyte.
RFE	Relative Faraday efficiency.

References

1. Kawashima, K.; Márquez, R.A.; Smith, L.A.; Vaidyula, R.R.; Carrasco-Jaim, O.A.; Wang, Z.; Son, Y.J.; Cao, C.L.; Mullins, C.B. A Review of Transition Metal Boride, Carbide, Pnictide, and Chalcogenide Water Oxidation Electrocatalysts. *Chem. Rev.* **2023**, *123*, 12795–13208. [[CrossRef](#)] [[PubMed](#)]
2. Tong, W.; Forster, M.; Dionigi, F.; Drespe, S.; Erami, R.S.; Strasser, P.; Cowan, A.J.; Farràs, P. Electrolysis of low-grade and saline surface water. *Nat. Energy* **2020**, *5*, 367–377, Erratum in *Nat. Energy* **2021**, *6*, 935. [[CrossRef](#)]
3. Liu, T.; Zhao, Z.; Tang, W.; Chen, Y.; Lan, C.; Zhu, L.; Jiang, W.; Wu, Y.; Wang, Y.; Yang, Z.; et al. In-situ direct seawater electrolysis using floating platform in ocean with uncontrollable wave motion. *Nat. Commun.* **2024**, *15*, 5305. [[CrossRef](#)] [[PubMed](#)]
4. Zhang, S.; Wang, Y.; Li, S.; Wang, Z.; Chen, H.; Yi, L.; Chen, X.; Yang, Q.; Xu, W.; Wang, A.; et al. Concerning the stability of seawater electrolysis: A corrosion mechanism study of halide on Ni-based anode. *Nat. Commun.* **2023**, *14*, 4822. [[CrossRef](#)]

5. Lim, T.; Jung, G.Y.; Kim, J.H.; Park, S.O.; Park, J.; Kim, Y.-T.; Kang, S.J.; Jeong, H.Y.; Kwak, S.K.; Joo, S.H. Atomically dispersed Pt-N4 sites as efficient and selective electrocatalysts for the chlorine evolution reaction. *Nat. Commun.* **2020**, *11*, 412. [[CrossRef](#)] [[PubMed](#)]
6. Liu, D.; Cai, Y.; Wang, X.; Zhuo, Y.; Sui, X.; Pan, H.; Wang, Z. Innovations in electrocatalysts, hybrid anodic oxidation, and electrolyzers for enhanced direct seawater electrolysis. *Energy Environ. Sci.* **2024**, *17*, 6897–6942. [[CrossRef](#)]
7. Ma, T.; Xu, W.; Li, B.; Chen, X.; Zhao, J.; Wan, S.; Jiang, K.; Zhang, S.; Wang, Z.; Tian, Z.; et al. The Critical Role of Additive Sulfate for Stable Alkaline Seawater Oxidation on Nickel-Based Electrodes. *Angew. Chem. Int. Ed.* **2021**, *60*, 22740–22744. [[CrossRef](#)]
8. Xie, H.; Zhao, Z.; Liu, T.; Wu, Y.; Lan, C.; Jiang, W.; Zhu, L.; Wang, Y.; Yang, D.; Shao, Z. A membrane-based seawater electrolyser for hydrogen generation. *Nature* **2022**, *612*, 673–678. [[CrossRef](#)] [[PubMed](#)]
9. Abney, C.W.; Mayes, R.T.; Saito, T.; Dai, S. Materials for the Recovery of Uranium from Seawater. *Chem. Rev.* **2017**, *117*, 13935–14013. [[CrossRef](#)]
10. Xu, W.; Ma, T.; Chen, H.; Pan, D.; Wang, Z.; Zhang, S.; Zhang, P.; Bao, S.; Yang, Q.; Zhou, L.; et al. Scalable Fabrication of Cu₂S@NiS@Ni/NiMo Hybrid Cathode for High-Performance Seawater Electrolysis. *Adv. Funct. Mater.* **2023**, *33*, 2302263. [[CrossRef](#)]
11. Zou, X.; Zhang, Y. Noble metal-free hydrogen evolution catalysts for water splitting. *Chem. Soc. Rev.* **2015**, *44*, 5148–5180. [[CrossRef](#)] [[PubMed](#)]
12. Kirk, D.; Ledas, A. Precipitate formation during sea water electrolysis. *Int. J. Hydrogen Energy* **1982**, *7*, 925–932. [[CrossRef](#)]
13. Yi, L.; Chen, X.; Wen, Y.; Chen, H.; Zhang, S.; Yang, H.; Li, W.; Zhou, L.; Xu, B.; Xu, W.; et al. Solidophobic Surface for Electrochemical Extraction of High-Valued Mg(OH)₂ Coupled with H₂ Production from Seawater. *Nano Lett.* **2024**, *24*, 5920–5928. [[CrossRef](#)] [[PubMed](#)]
14. Johnson, E.R.; Keinan, S.; Mori-Sánchez, P.; Contreras-García, J.; Cohen, A.J.; Yang, W. Revealing Noncovalent Interactions. *J. Am. Chem. Soc.* **2010**, *132*, 6498–6506. [[CrossRef](#)] [[PubMed](#)]
15. Lu, X.; Pan, J.; Lovell, E.; Tan, T.H.; Ng, Y.H.; Amal, R. A sea-change: Manganese doped nickel/nickel oxide electrocatalysts for hydrogen generation from seawater. *Energy Environ. Sci.* **2018**, *11*, 1898–1910. [[CrossRef](#)]
16. Bennett, J. Electrodes for generation of hydrogen and oxygen from seawater. *Int. J. Hydrogen Energy* **1980**, *5*, 401–408. [[CrossRef](#)]
17. D’amore-Domenech, R.; Santiago, Ó.; Leo, T.J. Multicriteria analysis of seawater electrolysis technologies for green hydrogen production at sea. *Renew. Sustain. Energy Rev.* **2020**, *133*, 110166. [[CrossRef](#)]
18. Liang, J.; Cai, Z.; Li, Z.; Yao, Y.; Luo, Y.; Sun, S.; Zheng, D.; Liu, Q.; Sun, X.; Tang, B. Efficient bubble/precipitate traffic enables stable seawater reduction electrocatalysis at industrial-level current densities. *Nat. Commun.* **2024**, *15*, 2950. [[CrossRef](#)]
19. Liang, J.; Cai, Z.; He, X.; Luo, Y.; Zheng, D.; Sun, S.; Liu, Q.; Li, L.; Chu, W.; Alfaifi, S.; et al. Electroreduction of alkaline/natural seawater: Self-cleaning Pt/carbon cathode and on-site co-synthesis of H₂ and Mg hydroxide nanoflakes. *Chem* **2024**. [[CrossRef](#)]
20. Perea, D.E.; Arslan, I.; Liu, J.; Ristanović, Z.; Kovarik, L.; Arey, B.W.; Lercher, J.A.; Bare, S.R.; Weckhuysen, B.M. Determining the location and nearest neighbours of aluminium in zeolites with atom probe tomography. *Nat. Commun.* **2015**, *6*, 7589. [[CrossRef](#)] [[PubMed](#)]
21. Israelachvili, J.; Wennerström, H. Role of hydration and water structure in biological and colloidal interactions. *Nature* **1996**, *379*, 219–225. [[CrossRef](#)] [[PubMed](#)]
22. Zuo, K.; Zhang, X.; Huang, X.; Oliveira, E.F.; Guo, H.; Zhai, T.; Wang, W.; Alvarez, P.J.J.; Elimelech, M.; Ajayan, P.M.; et al. Ultrahigh resistance of hexagonal boron nitride to mineral scale formation. *Nat. Commun.* **2022**, *13*, 4523. [[CrossRef](#)]
23. Xiao, X.; Yang, L.; Sun, W.; Chen, Y.; Yu, H.; Li, K.; Jia, B.; Zhang, L.; Ma, T. Electrocatalytic Water Splitting: From Harsh and Mild Conditions to Natural Seawater. *Small* **2021**, *18*, 2105830. [[CrossRef](#)]
24. Dionigi, F.; Reier, T.; Pawolek, Z.; Glietz, M.; Strasser, P.P. Design Criteria, Operating Conditions, and Nickel–Iron Hydroxide Catalyst Materials for Selective Seawater Electrolysis. *ChemSusChem* **2016**, *9*, 962–972. [[CrossRef](#)]
25. Kuang, Y.; Kenney, M.J.; Meng, Y.; Hung, W.-H.; Liu, Y.; Huang, J.E.; Prasanna, R.; Li, P.; Li, Y.; Wang, L.; et al. Solar-driven, highly sustained splitting of seawater into hydrogen and oxygen fuels. *Proc. Natl. Acad. Sci. USA* **2019**, *116*, 6624–6629. [[CrossRef](#)] [[PubMed](#)]
26. He, D.; Yang, P.; Yang, K.; Qiu, J.; Wang, Z. Long-Lasting Hybrid Seawater Electrolysis Enabled by Anodic Mass Transport Intensification for Energy-Saving Hydrogen Production. *Adv. Funct. Mater.* **2024**. [[CrossRef](#)]
27. Liu, W.; Yu, J.; Li, T.; Li, S.; Ding, B.; Guo, X.; Cao, A.; Sha, Q.; Zhou, D.; Kuang, Y.; et al. Self-protecting CoFeAl-layered double hydroxides enable stable and efficient brine oxidation at 2 A cm⁻². *Nat. Commun.* **2024**, *15*, 4712. [[CrossRef](#)] [[PubMed](#)]
28. Liu, W.; Liu, W.; Yu, J.; Yu, J.; Sendeku, M.G.; Sendeku, M.G.; Li, T.; Li, T.; Gao, W.; Gao, W.; et al. Ferricyanide Armed Anodes Enable Stable Water Oxidation in Saturated Saline Water at 2 A/cm². *Angew. Chem. Int. Ed.* **2023**, *62*, e202309882. [[CrossRef](#)]
29. Mohili, R.; Hemanth, N.R.; Jin, H.; Lee, K.; Chaudhari, N. Emerging high entropy metal sulphides and phosphides for electrochemical water splitting. *J. Mater. Chem. A* **2023**, *11*, 10463–10472. [[CrossRef](#)]
30. Huang, C.; Zhou, Q.; Duan, D.; Yu, L.; Zhang, W.; Wang, Z.; Liu, J.; Peng, B.; An, P.; Zhang, J.; et al. The rapid self-reconstruction of Fe-modified Ni hydroxysulfide for efficient and stable large-current-density water/seawater oxidation. *Energy Environ. Sci.* **2022**, *15*, 4647–4658. [[CrossRef](#)]
31. Yu, L.; Wu, L.; McElhenny, B.; Song, S.; Luo, D.; Zhang, F.; Yu, Y.; Chen, S.; Ren, Z. Ultrafast room-temperature synthesis of porous S-doped Ni/Fe (oxy)hydroxide electrodes for oxygen evolution catalysis in seawater splitting. *Energy Environ. Sci.* **2020**, *13*, 3439–3446. [[CrossRef](#)]

32. Li, T.; Zhao, X.; Sendeku, M.G.; Zhang, X.; Xu, L.; Wang, Z.; Wang, S.; Duan, X.; Liu, H.; Liu, W.; et al. Phosphate-decorated Ni₃Fe-LDHs@CoPx nanoarray for near-neutral seawater splitting. *Chem. Eng. J.* **2023**, *460*, 141413. [[CrossRef](#)]
33. Song, H.J.; Yoon, H.; Ju, B.; Lee, D.-Y.; Kim, D.-W. Electrocatalytic Selective Oxygen Evolution of Carbon-Coated Na₂Co_{1-x}Fe_xP₂O₇ Nanoparticles for Alkaline Seawater Electrolysis. *ACS Catal.* **2019**, *10*, 702–709. [[CrossRef](#)]
34. Wu, L.; Yu, L.; Zhang, F.; McElhenny, B.; Luo, D.; Karim, A.; Chen, S.; Ren, Z. Heterogeneous Bimetallic Phosphide Ni₂P-Fe₂P as an Efficient Bifunctional Catalyst for Water/Seawater Splitting. *Adv. Funct. Mater.* **2020**, *31*, 2006484. [[CrossRef](#)]
35. Wang, Y.; Yang, Y.; Wang, X.; Li, P.; Shao, H.; Li, T.; Liu, H.; Zheng, Q.; Hu, J.; Duan, L.; et al. Electro-synthesized Co(OH)₂@CoSe with Co–OH active sites for overall water splitting electrocatalysis. *Nanoscale Adv.* **2020**, *2*, 792–797. [[CrossRef](#)] [[PubMed](#)]
36. Zhu, J.; Mao, B.; Wang, B.; Cao, M. The dynamic anti-corrosion of self-derived space charge layer enabling long-term stable seawater oxidation. *Appl. Catal. B Environ.* **2024**, *344*, 123658. [[CrossRef](#)]
37. Fan, R.; Liu, C.; Li, Z.; Huang, H.; Feng, J.; Li, Z.; Zou, Z. Ultrastable electrocatalytic seawater splitting at ampere-level current density. *Nat. Sustain.* **2024**, *7*, 158–167. [[CrossRef](#)]
38. Zhang, B.; Liu, S.; Zhang, S.; Cao, Y.; Wang, H.; Han, C.; Sun, J. High Corrosion Resistance of NiFe-Layered Double Hydroxide Catalyst for Stable Seawater Electrolysis Promoted by Phosphate Intercalation. *Small* **2022**, *18*, e2203852. [[CrossRef](#)]
39. Deng, P.; Liu, Y.; Liu, H.; Li, X.; Lu, J.; Jing, S.; Tsiakaras, P. Layered Double Hydroxides with Carbonate Intercalation as Ultra-Stable Anodes for Seawater Splitting at Ampere-Level Current Density. *Adv. Energy Mater.* **2024**, *14*, 2400053. [[CrossRef](#)]
40. Corrigan, D.A.; Bendert, R.M. Effect of Coprecipitated Metal Ions on the Electrochemistry of Nickel Hydroxide Thin Films: Cyclic Voltammetry in 1M KOH. *J. Electrochem. Soc.* **1989**, *136*, 723–728. [[CrossRef](#)]
41. Lu, X.; Zhao, C. Electrodeposition of hierarchically structured three-dimensional nickel–iron electrodes for efficient oxygen evolution at high current densities. *Nat. Commun.* **2015**, *6*, 6616. [[CrossRef](#)] [[PubMed](#)]
42. Weng, L.T.; Bertrand, P.; Stone-Masui, J.H.; Stone, W.E.E. ToF SIMS study of the desorption of emulsifiers from polystyrene latexes. *Surf. Interface Anal.* **1994**, *21*, 387–394. [[CrossRef](#)]
43. Zhou, D.; Cai, Z.; Bi, Y.; Tian, W.; Luo, M.; Zhang, Q.; Xie, Q.; Wang, J.; Li, Y.; Kuang, Y.; et al. Effects of redox-active interlayer anions on the oxygen evolution reactivity of NiFe-layered double hydroxide nanosheets. *Nano Res.* **2018**, *11*, 1358–1368. [[CrossRef](#)]
44. Guo, L.; Chi, J.; Cui, T.; Zhu, J.; Xia, Y.; Guo, H.; Lai, J.; Wang, L. Phosphorus Defect Mediated Electron Redistribution to Boost Anion Exchange Membrane-Based Alkaline Seawater Electrolysis. *Adv. Energy Mater.* **2024**, *14*, 2400975. [[CrossRef](#)]
45. Zhou, Y.-N.; Wang, F.-L.; Dou, S.-Y.; Shi, Z.-N.; Dong, B.; Yu, W.-L.; Zhao, H.-Y.; Wang, F.-G.; Yu, J.-F.; Chai, Y.-M. Motivating high-valence Nb doping by fast molten salt method for NiFe hydroxides toward efficient oxygen evolution reaction. *Chem. Eng. J.* **2021**, *427*, 131643. [[CrossRef](#)]
46. Liu, X.; Chi, J.; Mao, H.; Wang, L. Principles of Designing Electrocatalyst to Boost Reactivity for Seawater Splitting. *Adv. Energy Mater.* **2023**, *13*, 2301438. [[CrossRef](#)]
47. Shi, Y.; Du, W.; Zhou, W.; Wang, C.; Lu, S.; Lu, S.; Zhang, B. Unveiling the Promotion of Surface-Adsorbed Chalcogenate on the Electrocatalytic Oxygen Evolution Reaction. *Angew. Chem. Int. Ed.* **2020**, *59*, 22470–22474. [[CrossRef](#)] [[PubMed](#)]
48. Jagger, B.; Pasta, M. Solid electrolyte interphases in lithium metal batteries. *Joule* **2023**, *7*, 2228–2244. [[CrossRef](#)]
49. Zhang, L.; Wang, Z.; Qiu, J. Energy-Saving Hydrogen Production by Seawater Electrolysis Coupling Sulfion Degradation. *Adv. Mater.* **2022**, *34*, 2109321. [[CrossRef](#)]
50. Qiu, Z.; Ma, Y.; Edvinsson, T. In operando Raman investigation of Fe doping influence on catalytic NiO intermediates for enhanced overall water splitting. *Nano Energy* **2019**, *66*, 104118. [[CrossRef](#)]
51. Liu, W.; Huang, Y.-L.; Yin, Z.-L.; Ding, Z.-Y. Investigation on the decomposition process of sodium aluminate solution by spectroscopic and theoretical calculation. *J. Mol. Liq.* **2018**, *261*, 115–122. [[CrossRef](#)]
52. Ram, S. Infrared spectral study of molecular vibrations in amorphous, nanocrystalline and AlO(OH)· α H₂O bulk crystals. *Infrared Phys. Technol.* **2001**, *42*, 547–560. [[CrossRef](#)]
53. Kang, X.; Yang, F.; Zhang, Z.; Liu, H.; Ge, S.; Hu, S.; Li, S.; Luo, Y.; Yu, Q.; Liu, Z.; et al. A corrosion-resistant RuMoNi catalyst for efficient and long-lasting seawater oxidation and anion exchange membrane electrolyzer. *Nat. Commun.* **2023**, *14*, 3607. [[CrossRef](#)] [[PubMed](#)]
54. Haq, T.U.; Haik, Y. Strategies of Anode Design for Seawater Electrolysis: Recent Development and Future Perspective. *Small Sci.* **2022**, *2*, 2200030. [[CrossRef](#)]
55. Lu, Y.; Clayton, C.; Brooks, A. A bipolar model of the passivity of stainless steels—II. The influence of aqueous molybdate. *Corros. Sci.* **1989**, *29*, 863–880. [[CrossRef](#)]
56. Sakashita, M.; Sato, N. The effect of molybdate anion on the ion-selectivity of hydrous ferric oxide films in chloride solutions. *Corros. Sci.* **1977**, *17*, 473–486. [[CrossRef](#)]
57. Zhou, L.; Guo, D.; Wu, L.; Guan, Z.; Zou, C.; Jin, H.; Fang, G.; Chen, X.; Wang, S. A restricted dynamic surface self-reconstruction toward high-performance of direct seawater oxidation. *Nat. Commun.* **2024**, *15*, 2481. [[CrossRef](#)]
58. Zhang, S.; Xu, W.; Chen, H.; Yang, Q.; Liu, H.; Bao, S.; Tian, Z.; Slavcheva, E.; Lu, Z. Progress in Anode Stability Improvement for Seawater Electrolysis to Produce Hydrogen. *Adv. Mater.* **2024**, *36*, e2311322. [[CrossRef](#)]
59. Duan, X.; Sha, Q.; Li, P.; Li, T.; Yang, G.; Liu, W.; Yu, E.; Zhou, D.; Fang, J.; Chen, W.; et al. Dynamic chloride ion adsorption on single iridium atom boosts seawater oxidation catalysis. *Nat. Commun.* **2024**, *15*, 1973. [[CrossRef](#)]

60. Shen, W.; Hu, T.; Liu, X.; Zha, J.; Meng, F.; Wu, Z.; Cui, Z.; Yang, Y.; Li, H.; Zhang, Q.; et al. Defect engineering of layered double hydroxide nanosheets as inorganic photosensitizers for NIR-III photodynamic cancer therapy. *Nat. Commun.* **2022**, *13*, 3384. [[CrossRef](#)] [[PubMed](#)]
61. Mefford, J.T.; Akbashev, A.R.; Kang, M.; Bentley, C.L.; Gent, W.E.; Deng, H.D.; Alsem, D.H.; Yu, Y.-S.; Salmon, N.J.; Shapiro, D.A.; et al. Correlative operando microscopy of oxygen evolution electrocatalysts. *Nature* **2021**, *593*, 67–73. [[CrossRef](#)] [[PubMed](#)]
62. Zhang, J.; Liu, J.; Xi, L.; Yu, Y.; Chen, N.; Sun, S.; Wang, W.; Lange, K.M.; Zhang, B. Single-Atom Au/NiFe Layered Double Hydroxide Electrocatalyst: Probing the Origin of Activity for Oxygen Evolution Reaction. *J. Am. Chem. Soc.* **2018**, *140*, 3876–3879. [[CrossRef](#)] [[PubMed](#)]
63. Guo, J.; Zheng, Y.; Hu, Z.; Zheng, C.; Mao, J.; Du, K.; Jaroniec, M.; Qiao, S.-Z.; Ling, T. Direct seawater electrolysis by adjusting the local reaction environment of a catalyst. *Nat. Energy* **2023**, *8*, 264–272. [[CrossRef](#)]
64. Kunitatsu, K.; Yoda, T.; Tryk, D.A.; Uchida, H.; Watanabe, M. In situ ATR-FTIR study of oxygen reduction at the Pt/Nafion interface. *Phys. Chem. Chem. Phys.* **2009**, *12*, 621–629. [[CrossRef](#)]
65. Zhu, S.; Qin, X.; Yao, Y.; Shao, M. pH-Dependent Hydrogen and Water Binding Energies on Platinum Surfaces as Directly Probed through Surface-Enhanced Infrared Absorption Spectroscopy. *J. Am. Chem. Soc.* **2020**, *142*, 8748–8754. [[CrossRef](#)]
66. Deng, W.; Zhang, L.; Li, L.; Chen, S.; Hu, C.; Zhao, Z.-J.; Wang, T.; Gong, J. Crucial Role of Surface Hydroxyls on the Activity and Stability in Electrochemical CO₂ Reduction. *J. Am. Chem. Soc.* **2019**, *141*, 2911–2915. [[CrossRef](#)]
67. Kitano, S.; Noguchi, T.G.; Nishihara, M.; Kamitani, K.; Sugiyama, T.; Yoshioka, S.; Miwa, T.; Yoshizawa, K.; Staykov, A.; Yamauchi, M. Heterointerface Created on Au-Cluster-Loaded Unilamellar Hydroxide Electrocatalysts as a Highly Active Site for the Oxygen Evolution Reaction. *Adv. Mater.* **2022**, *34*, e2110552. [[CrossRef](#)] [[PubMed](#)]
68. Yang, X.; Nash, J.; Oliveira, N.; Yan, Y.; Xu, B. Understanding the pH Dependence of Underpotential Deposited Hydrogen on Platinum. *Angew. Chem. Int. Ed.* **2019**, *58*, 17718–17723. [[CrossRef](#)]
69. Lu, Z.; Xu, W.; Zhu, W.; Yang, Q.; Lei, X.; Liu, J.; Li, Y.; Sun, X.; Duan, X. Three-dimensional NiFe layered double hydroxide film for high-efficiency oxygen evolution reaction. *Chem. Commun.* **2014**, *50*, 6479–6482. [[CrossRef](#)]
70. Choudhury, M.R.; Anwar, N.; Jassby, D.; Rahaman, M.S. Fouling and wetting in the membrane distillation driven wastewater reclamation process—A review. *Adv. Colloid Interface Sci.* **2019**, *269*, 370–399. [[CrossRef](#)] [[PubMed](#)]
71. Ahmad, N.A.; Goh, P.S.; Yogarathinam, L.T.; Zulhairun, A.K.; Ismail, A.F. Current advances in membrane technologies for produced water desalination. *Desalination* **2020**, *493*, 114643. [[CrossRef](#)]
72. Ren, Y.; Fan, F.; Zhang, Y.; Chen, L.; Wang, Z.; Li, J.; Zhao, J.; Tang, B.; Cui, G. A Dual-Cation Exchange Membrane Electrolyzer for Continuous H₂ Production from Seawater. *Adv. Sci.* **2024**, *11*, 2401702. [[CrossRef](#)] [[PubMed](#)]
73. Liang, H.-Q.; Hung, W.-S.; Yu, H.-H.; Hu, C.-C.; Lee, K.-R.; Lai, J.-Y.; Xu, Z.-K. Forward osmosis membranes with unprecedented water flux. *J. Membr. Sci.* **2017**, *529*, 47–54. [[CrossRef](#)]
74. Guo, J.; Zhang, Y.; Zavabeti, A.; Chen, K.; Guo, Y.; Hu, G.; Fan, X.; Li, G.K. Hydrogen production from the air. *Nat. Commun.* **2022**, *13*, 5046. [[CrossRef](#)] [[PubMed](#)]
75. He, W.; Li, X.; Tang, C.; Zhou, S.; Lu, X.; Li, W.; Li, X.; Zeng, X.; Dong, P.; Zhang, Y.; et al. Materials Design and System Innovation for Direct and Indirect Seawater Electrolysis. *ACS Nano* **2023**, *17*, 22227–22239. [[CrossRef](#)]
76. Liu, R.-T.; Xu, Z.-L.; Li, F.-M.; Chen, F.-Y.; Yu, J.-Y.; Yan, Y.; Chen, Y.; Xia, B.Y. Recent advances in proton exchange membrane water electrolysis. *Chem. Soc. Rev.* **2023**, *52*, 5652–5683. [[CrossRef](#)]
77. Keane, T.P.; Veroneau, S.S.; Hartnett, A.C.; Nocera, D.G. Generation of Pure Oxygen from Briny Water by Binary Catalysis. *J. Am. Chem. Soc.* **2023**, *145*, 4989–4993. [[CrossRef](#)]
78. Li, M.; Xie, P.; Yu, L.; Luo, L.; Sun, X. Bubble Engineering on Micro-/Nanostructured Electrodes for Water Splitting. *ACS Nano* **2023**, *17*, 23299–23316. [[CrossRef](#)]
79. Xu, W.; Lu, Z.; Sun, X.; Jiang, L.; Duan, X. Superwetting Electrodes for Gas-Involving Electrocatalysis. *Accounts Chem. Res.* **2018**, *51*, 1590–1598. [[CrossRef](#)]
80. Sun, Z.; Wang, G.; Koh, S.W.; Ge, J.; Zhao, H.; Hong, W.; Fei, J.; Zhao, Y.; Gao, P.; Miao, H.; et al. Solar-Driven Alkaline Water Electrolysis with Multifunctional Catalysts. *Adv. Funct. Mater.* **2020**, *30*, 2002138. [[CrossRef](#)]
81. Brauns, J.; Turek, T. Alkaline Water Electrolysis Powered by Renewable Energy: A Review. *Processes* **2020**, *8*, 248. [[CrossRef](#)]
82. Zhang, F.; Zhou, J.; Chen, X.; Zhao, S.; Zhao, Y.; Tang, Y.; Tian, Z.; Yang, Q.; Slavcheva, E.; Lin, Y.; et al. The Recent Progresses of Electrodes and Electrolyzers for Seawater Electrolysis. *Nanomaterials* **2024**, *14*, 239. [[CrossRef](#)] [[PubMed](#)]
83. Hu, H.; Zhang, Z.; Liu, L.; Che, X.; Wang, J.; Zhu, Y.; Attfield, J.P.; Yang, M. Efficient and durable seawater electrolysis with a V₂O₃-protected catalyst. *Sci. Adv.* **2024**, *10*, eadn7012. [[CrossRef](#)]
84. Wan, L.; Pang, M.; Le, J.; Xu, Z.; Zhou, H.; Xu, Q.; Wang, B. Oriented intergrowth of the catalyst layer in membrane electrode assembly for alkaline water electrolysis. *Nat. Commun.* **2022**, *13*, 7956. [[CrossRef](#)]

Disclaimer/Publisher's Note: The statements, opinions and data contained in all publications are solely those of the individual author(s) and contributor(s) and not of MDPI and/or the editor(s). MDPI and/or the editor(s) disclaim responsibility for any injury to people or property resulting from any ideas, methods, instructions or products referred to in the content.